MDPI

Entanglements of Macromolecules and Their Influence on Rheological and Mechanical Properties of Polymers

Andrzej Pawlak *(D) and Justyna Krajenta (D)

Centre of Molecular and Macromolecular Studies, Polish Academy of Sciences, 90-363 Lodz, Poland;
justyna.krajenta@cbmm.lodz.pl
* Correspondence: andrzej.pawlak@cbmm.lodz.pl

Abstract: Flexible macromolecules easily become entangled with neighboring macromolecules. The resulting network determines many polymer properties, including rheological and mechanical properties. Therefore, a number of experimental and modeling studies were performed to describe the relationship between the degree of entanglement of macromolecules and polymer properties. The introduction presents general information about the entanglements of macromolecule chains, collected on the basis of studies of equilibrium entangled polymers. It is also shown how the density of entanglements can be reduced. The second chapter presents experiments and models leading to the description of the movement of a single macromolecule. The next part of the text discusses how the rheological properties change after partial disentangling of the polymer. The results on the influence of the degree of chain entanglement on mechanical properties are presented.

Keywords: entanglements; rheology of polymers; mechanical properties; semi-crystalline polymers

1. Introduction

Macromolecules based on carbon–carbon bonds in the main chain are long and flexible, allowing them to take on different configurations in space, from a straightened linear to an entangled coil. In the polymer, each macromolecule is surrounded by a number of other macromolecules. Because of this, macromolecules can interpenetrate and form topological entanglements, usually in the form of a loop of one macromolecule around another macromolecule [1]. The presence of entanglements, acting as physical knots in the macromolecular network, limits the possibilities for movement of macromolecules, as well as their relaxation. It is not surprising that the presence of entanglements affects many polymer properties, among them rheological and mechanical [2]. In particular, because they are present in the molten polymer, in the polymer solution, and in the amorphous phase of the solid polymer. The exception is the crystalline phase of the polymer, where the crystal structure does not allow entanglements to be accommodated and they are rejected outside the crystal volume.

The presence of entanglements was discovered many years ago in rheological studies. Berry and Fox [3] observed that the dependence of zero shear viscosity η_0 on the molecular weight of the polymer M changes from a certain molecular weight. It is proportional to $\eta_0 \sim M$, for low molecular weights and as $\eta_0 \sim M^{3.4}$ for higher molecular weights. The reason for this change is the entanglement of longer macromolecules.

The entanglements were also identified in solid amorphous materials, which above a glass transition can exhibit large deformation and elastic response. Such behavior is explained by the stretching and relaxation of the network of entangled macromolecules. Amorphous polymer or the amorphous component of semi-crystalline polymer at elevated temperatures behaves similarly to rubber. However, in rubbers, the macromolecular network is the result of chemical cross-linking. The entanglements act as physical cross-links, equivalent to chemical cross-links in rubber [4]. The influence of entanglements in

the melt and in the elastic solid polymer on the properties can be described by equations of similar form. In the case of melt rheology, the relevant equation is of the form:

$$G_N^0 = \frac{g\rho RT}{M_e} \tag{1}$$

where G_N^0 is the shear modulus in the rubbery plateau region, R is the gas constant, T is the temperature, ρ is the density of the polymer, g is a coefficient equal to 1.0 [5] or 0.8 [6] and M_e is the molecular mass between the nodes of network, in this case between the entanglements.

A similar equation, based on the classical theory of elasticity [7], describes the high elastic properties of a solid polymer:

$$G_e = \rho_r RT/M_r \tag{2}$$

where G_e is the shear modulus, ρ_r is the density of the rubber, and M_r is the molecular mass between the network nodes [8–10]. There are other models that can be used to describe the properties, such as the phantom network model, leading to the modified Equation (2):

$$G_e = \left(1 - \frac{2}{f}\right)\frac{\rho_r RT}{M_r} \tag{3}$$

where f is the functionality, i.e., the number of polymer arms that are connected to a cross-linking junction [11].

From Equation (1), it can be concluded that the best parameter characterizing an entangled network of linear macromolecules is the molecular mass between the entanglements. The entanglement density, sometimes used instead of M_e, is proportional to $1/M_e$. It is generally accepted that each type of polymer has its own M_e value. This value depends mainly on the architecture of the macromolecular chain. Calculations for monodisperse polybutadiene, polyisoprene, and polystyrene showed that M_e is independent of the weight average molecular weight M_w and is also independent of polydispersity (i.e., the M_w/M_n ratio, where M_n is the number average molecular weight) [12]. These statements should be treated with caution due to the limited amount of data available. Some studies of mechanical properties show that in semi-crystalline polymers M_e can depend on M_w (see Section 4.1 for details). It was also found that M_e depends on the tacticity of the macromolecules [13,14]. Since entanglements may not be uniformly distributed along the macromolecule chain, the reported M_e values should be treated as averages.

There is a second parameter, important for characterizing entanglements, which is the critical molecular mass M_c. When the molecular weight of the polymer exceeds this value, the relationship between the zero shear viscosity η_0 and the molecular weight changes from $\eta_0 \sim M_w$ to $\eta_0 \sim M_w^{3.4}$. M_c is greater than M_e, and the ratio of their values is in the range of 1.0–3.5 [15].

Commercial polymers, typically processed, are in an equilibrium entangled state [13]. However, there are known methods to reduce entanglement. This allows for a deeper examination of the relationship between entanglement and polymer properties. Three groups of disentangling methods can be distinguished [16]: by dissolution and freezing (often called freeze-drying) [17–22], by polymerization with crystallization [23], by shearing of melt [24–28]. The dissolution is a method that can be used on a laboratory scale for any polymer. It is known that in a dilute polymer solution, the number of contacts between macromolecules, which then have the coil shape, decreases as the concentration of the solution decreases [29]. In a very dilute solution, one can even expect complete disentanglement and separation of the macromolecule chains. However, for practical reasons, it is usually better to have the polymer only partially disentangled, since chain entanglements are necessary to maintain the continuity of the amorphous phase of the solidified polymer under the action of force.

To use a polymer as a material, it is necessary to maintain the disentanglement state in the solid polymer. This can be performed by rapidly freezing the solution, for example using liquid nitrogen, and then removing the solvent, for example by sublimation [30–34]. There are variants of the solvent method in which disentanglement stabilization is achieved by crystallization from the hot solution or by adding a non-solvent to the frozen solution [35–40].

It is possible to disentangle the polymer during its polymerization [23,41–43]. Therefore, special catalysts and conditions are needed to separate the polymerization sites and enable immediate crystallization of the growing chains without entanglement. This approach has been mainly used for the polymerization of ultra-high molecular weight polyethylene (UHMWPE) [44–49].

Recently, a group of methods has been developed based on the observation that in polymer subjected to shear flow, there is not only orientation but also some disentanglement of macromolecules. In order to achieve disentanglement, the processing equipment has been modified to obtain different shear states, including pulsation or the addition of an elongation flow component [50–55]. This raises the prospect of commercial production of the partially disentangled polymers.

The next chapter briefly presents observations of the shape and dynamics of a macromolecule in the presence of other macromolecules, studied using neutron scattering, and a successful theoretical approach to describing the motion of macromolecule chains using a tube model.

Sections 3 and 4 describe the rheological and mechanical properties of polymers from the perspective of entanglement research. Each section provides background based on the results of older experiments and results reported in the last few years. Most entanglement research has been focused on homopolymers. Not very often, especially when talking about entanglement reduction, polymer blends or polymer composites are analyzed.

2. Macromolecule in the Environment of Other Macromolecules

The plateau in the storage modulus G_N^0 observed for the molten polymer is similar to the plateau observed for cross-linked rubbers. This led to the conclusion that in the molten polymer, there is a network of macromolecules connected by nodes, which are entanglements. Therefore, research on the shape of macromolecules and the dynamics of chain motion in the molten and solid polymers was initiated. Almost simultaneously, the development of theoretical models, with the support of computer calculations, and the search for new experimental methods were addressed.

The results of rheological research have stimulated attempts to describe the observed behavior theoretically. One of the first widely known was the Rouse model of chain motion, based on the approximation of a chain by a set of balls connected by springs. This model successfully described the properties of low-molecular-weight polymers but was less effective for high-molecular-weight polymers [56]. The approach proposed by DeGennes was much more successful [57]. He proposed the description in which a macromolecule moves inside a virtual tube, created by other macromolecules, and the movement is similar to that of a snake (Figure 1). This is known as the reptation concept, and the descriptive model proposed by Doi and Edwards [58] is known as the tube model. The dynamics of the chain are characterized by the time of diffusion through the tube [59,60]. Using the model, it was possible to predict changes in η_0 with M, but in the first version, an exponent of 3.0 was proposed instead of the experimentally found exponent of 3.4.
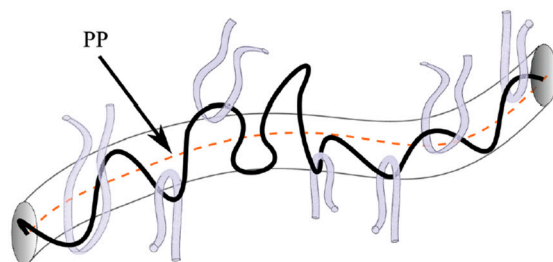
Figure 1. Virtual tube around the polymer chain. The centerline of the tube is referred to as primitive path (PP). The movement of chain in the direction of primitive path is possible, but transverse motion is restricted by the surrounding chains. Reproduced with permission from ref. [61]. Copyright 2020. Royal Society of Chemistry.

The development of the tube model by many authors has reduced this and other weaknesses of the model [6,59,62–66]. Modifications regarding contour length fluctuation [67], accounting for the dynamical variation of the primitive chain length [68], tube dilatation [69], and constraint release [70], accounting for the dynamics of the tube itself [68], have compensated for discrepancies between experimental results and the theory describing them. The success of the theory for the linear entangled polymers resulted in proposals to use the model for other architectures, such as mixtures of star and linear polymers [71], or long-chain branches [72]. The tube model is applied not only for polymer melts but also for the description of the dynamics of rubber elasticity [73]. The analysis of the reptation time τ_d, i.e., time of diffusion along the tube length, shows that it is generally not short, since it depends on $M^{3.4}$ through the zero shear viscosity η_0 [74]:

$$\tau_d = 20\, M_e\, \eta_0 / (\pi^2\, R\, T\, \rho) \tag{4}$$

When polyethylene has M = 4000 kg/mol, the reptation time is about 2 h [75], while reducing the molecular weight to M = 50 kg/mol shortens this time to 15 min. A more detailed description of tube model variants and their application can be found in the literature [76,77].

The search for experimental techniques suitable at the nanoscale focused on scattering methods. For dense polymers, light scattering, useful for studying dilute solutions, could not be used. Fortunately, small-angle neutron scattering (SANS) has just been developed to a level that made it possible to apply this method to the study of polymers. Neutron scattering results from the interactions of neutrons with the atomic nuclei. In the experiment, a collimated, monochromatic neutron beam hits the sample, and the scattering is monitored by a 2D detector [78]. The utility of SANS for polymer testing comes from both its coverage of large lengths and time scales and its ability to apply contrast to the polymer under study by introducing deuterated molecules [79].

The results of the first polymer studies using SANS were published in 1973. Early studies confirmed the random coil conformation of polymer chains in both molten and glassy polymers [80,81]. The SANS technique was used to determine the actual radius of gyration R_g of the chain in the bulk state. The dimension of macromolecules in a bulk polymer sample can be characterized by the value of the K coefficient, which depends on the molecular weight by $K = (R_g{}^2 / M_w)^{0.5}$ [82]. Typical K values for polymers range from 0.028 to 0.046 nm·mol$^{0.5}$/g$^{0.5}$ [83]. This means, for example, that molten polyethylene with $M_w = 10^5$ g/mol has $R_g = 14$ nm. Calculations show that a single macromolecular coil has a density of less than 1% of the volume density of the polymer, which indicates that the empty space inside it is filled with fragments of other macromolecules [84].

Quasi-elastic neutron scattering can be used to study the dynamics of polymers at different length scales [85]. At the large-scale dynamics, the observable processes are the chain diffusion, the reptation, and the Rouse dynamics. These processes control the rheological properties of the polymer [86]. The corresponding length scale where the topological confinement caused by interpenetrating coils dominates is above 10 nm. Typical

time scales for processes involving the entire macromolecule are nanoseconds or more [79]. Studies of polyethylene using an ultra-high-resolution spectrometer have confirmed that the observed changes in the dynamic structure factor are consistent with the reptation model [87]. The subject of studies with the application of contrast is not only the dynamics of individual chains in the melt but also their fragments, such as ends or branch points [88].

Nowadays, there is a tendency to increase the complexity of the investigated system [86,89]. Computer simulations, such as molecular dynamic simulation, are very helpful in the interpretation of scattering results [90]. The polymer dynamics in nanocomposites in the presence of movement confinement is an example of modern research with the use of the neutron spin echo technique [78,91–93]. Schneider et al. [94], studying poly(ethylene propylene) with silica, found that the confinement length, i.e., the tube diameter, decreased with silica contents, but the entanglement density was reduced at high nanofiller content. Nusser et al. [95] analyzed two relaxation processes associated with reptation, i.e., constraint release and contour length fluctuations.

From the above brief review of the literature, it appears that the SANS data support the tube model of entangled macromolecule motion.

3. Rheological Properties of Molten Polymers

3.1. Methods for Characterizing Entanglements

To describe the entanglement state using Equation (1), it is necessary to know the rheological moduli, obtained by measuring linear viscoelastic properties in an oscillatory shear experiment, performed over a wide range of frequencies and temperatures. In this experiment, the storage modulus G' and the loss modulus G'' are usually determined. The G_N^0 modulus in Equation (1), necessary to calculate M_e, is the value of the storage modulus at the frequency at which the loss modulus reaches its minimum [12]. This is shown in Figure 2a. Unfortunately, this classic approach often cannot be applied due to a lack of data for some high frequencies or simply the absence of a visible G'' minimum. For this reason, a number of other methods have been developed to characterize entanglements [12,13,96,97]. For example, if the minimum of the G'' modulus is poorly visible, as in the case of polydisperse polymers, the minimum of the $\tan \delta = G''/G'$ value can be taken as the position in the frequency to read G_N^0, but this criterion is more arbitrary [12,97].
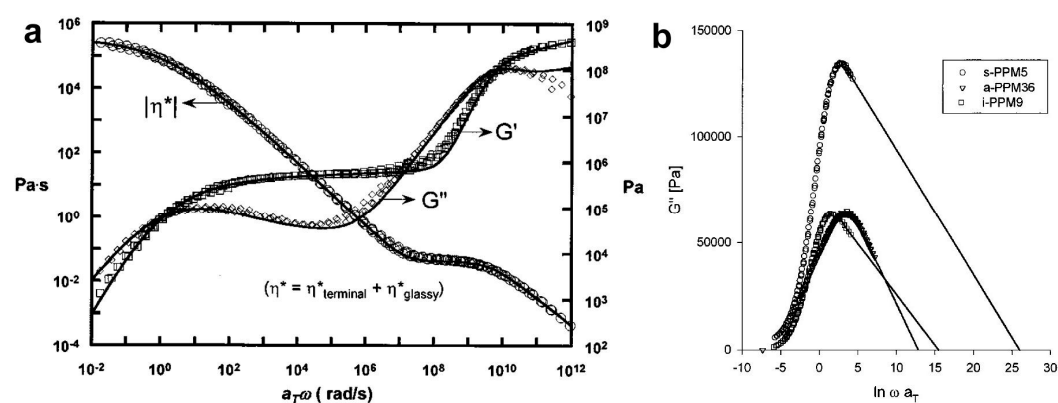

Figure 2. (**a**) Master curves for polylactide (PLA) sample showing nearly 14 decades in frequency obtained via time–temperature superposition. η^* is the complex viscosity, which is the sum of terminal ($\eta^*_{terminal}$) and glassy (η^*_{glassy}) components. Reproduced with permission from ref. [98]. Copyright 2005. The Society of Rheology. (**b**) Example of using the integral method to calculate the G_N^0 modulus from the area under the G'' peak, when some data are unavailable. The curves represent three polypropylenes. $\omega \times a_T$ is a reduced angular frequency. Reproduced with permission from ref. [13]. Copyright 1998. American Chemical Society.

An approach for determining M_e that is increasingly used is to calculate G_N^0 using the numerical integration of the area over the terminal relaxation peak of $G''(\omega)$. This

method, sometimes called the integral method, can be used for monodisperse polymers. The equation useful in G_N^0 calculation has the form [99]:

$$G_N^0 = 2\pi \int_{-\infty}^{\infty} G''(\omega) d\ln\omega \qquad (5)$$

In many cases, however, data about G'' are missing at high frequencies. For this reason, it was proposed to use a linear approximation for the missing data and then perform calculations in accordance with Equation (5) [13]. The application of the numerical integration to various polypropylenes is shown in Figure 2b.

A similar approach has been proposed for highly polydisperse materials, in which the terminal relaxation spectrum is broad, and the loss modulus peak is usually not recorded in its entirety. Therefore, assuming the symmetric shape of the G'' peak, calculations can be performed by taking a doubled peak area from the origin to the frequency corresponding to the maximum [12,97,100].

The method, now called the maximum method, was by Raju et al. [101]. If the chain dispersion is narrow and chains are long, the plateau modulus G_N^0 can be calculated from equation:

$$G_N^0 = 3.56\, G''_{max} \qquad (6)$$

where G''_{max} is the maximum of G'' modulus.

For many polymers, the presence of a cross-over point where G' and G'' are equal is observed [18] (Figure 3). Some researchers prefer to characterize entanglements by specifying this cross-over point, especially in the case of high polydispersity or when the polymer is semicrystalline [12]. It should be mentioned that the inverse values of the dynamic moduli at their intersection $G' = G''$ characterize the polydispersity of the samples [102] and that the cross-over frequency shifts to lower values with molecular weight [103]. To determine the level of entanglements, attempts are being made to use both the cross-over modulus G_x and the cross-over frequency ω_x.
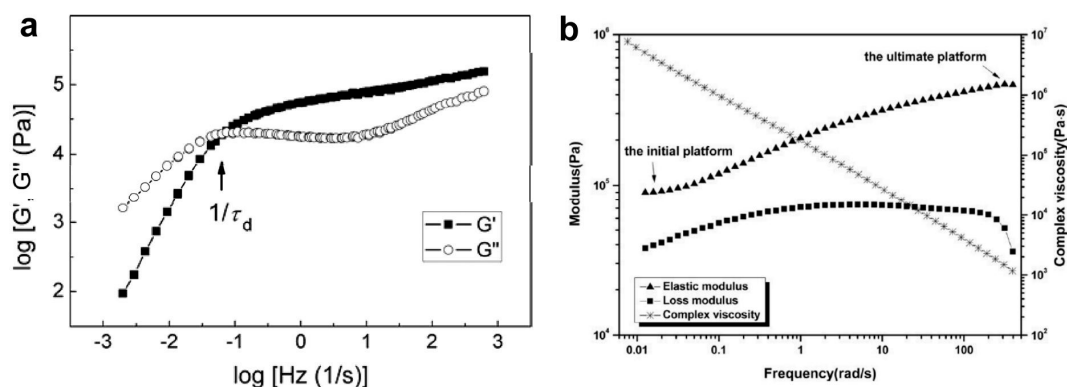

Figure 3. (**a**) Storage and loss modulus as a function of frequency at 150 °C of the bulk polystyrene (PS) sample. τ_d is the linear viscoelastic relaxation time. Reproduced with permission from ref. [18]. Copyright 2012. American Chemical Society. (**b**) Results of a dynamic frequency sweep experiment of a disentangled ultra-high molecular weight polyethylene (UHMWPE) sample, performed at temperature of 160 °C. There is no cross-over point. Reproduced with permission from ref. [104]. Copyright 2015. Springer Nature (Berlin, Germany).

Wu [97] and Nobile and Cochini [105] stated that the relationship between the cross-over modulus G_x and the plateau modulus G_N^0 should have the general form of:

$$\log\left(G_N^0 / G_x\right) = f(M_w, M_n, M_z) \qquad (7)$$

where M_w, M_n, M_z are weight-averaged, number-averaged, and z-averaged molecular weights, respectively. When the polydispersity of polymer is lower than 3, the Equation (7) has the form [97]:

$$\log (G_N^0/G_x) = 0.38 + 2.63 \log(M_w/M_n)/(1 + 2.45 \log(M_w/M_n)) \tag{8}$$

According to Equation (8), the cross-over modulus is a measure of entanglement. Higher values of G_x mean a higher density of entanglements.

Krajenta et al. [106] analyzed changes in the cross-over frequency as a function of the annealing time for differently entangled polypropylenes (PP) (Figure 4). It was observed that at the beginning of annealing, a higher frequency corresponded to a lower density of entanglements. This was consistent with the equation proposed by Martins et al. [107] linking ω_x with the number of entanglements per macromolecule $Z = M/M_e$:

$$1/\omega_x \approx \tau_R Z \tag{9}$$

where τ_R is the Rouse relaxation time, which depends on the chain length to the second power [108]. $1/\omega_x$ is equal to the reptation time [12,109]. As the annealing time increased, the cross-over point shifted toward higher frequencies, reaching a plateau. This would be interpreted as re-entanglement if, surprisingly, this was not also observed for equilibrium-entangled PP. The reason for the behavior observed with annealing time is not clear, because from other experiments for the same materials, the time of re-entanglement for the most disentangled PP was about 2 h, not 45 min, after which the plateau visible in Figure 3 was reached [106].
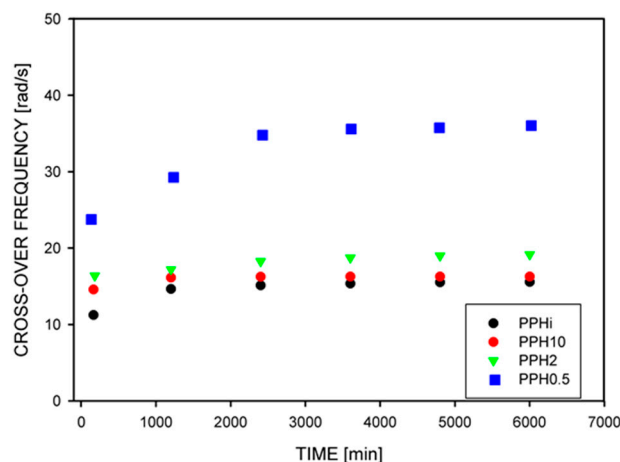

Figure 4. Changes in the cross-over frequency with annealing time at 185 °C. PPHi means equilibrium entangled polypropylene. PPH10, PPH2, and PPH0.5 are partially disentangled polypropylenes obtained by dissolving in xylene with concentration of 10, 2, and 0.5 wt.%, respectively. Reproduced with permission from ref. [106]. Copyright 2019. Elsevier (Amsterdam, The Netherlands).

It seems that the cross-over modulus, rather than the cross-over frequency, can be used to compare changes in the entangled state of a single polymer when other methods are not available. Sometimes the cross-over point does not exist (see Figure 3b), as in the case of a certain type of disentangled UHMWPE studied by Li et al. [104]. The absence of the cross-over point was interpreted as the absence of entanglement.

The molecular masses between entanglements, determined for equilibrium entangled polymers by the methods described above, are summarized in Table 1. For comparison, information on the critical molecular masses is also included. Two conclusions about M_e can be drawn from the data in Table 1. First, there is a scattering of results obtained in different laboratories. Second, the attempt to find a universal relationship between tacticity

and M_e has not been successful. It is also worth noting that many polymers have been characterized so far.

Table 1. Molecular masses between entanglements and critical molecular masses.

Polymer	M_e [g/mol]	M_c [g/mol]	Literature Sources
Polyethylene	830–2600	2800–3480	[13,15,97,110–114]
Poly(ethylene oxide)	1600–2200	5870	[15,97,112]
Polyisobutylene	6900–10,500	13,100–17,000	[15,97]
Polylactide	4000–10,500	9000–10,000	[98,115–117]
Syndiotactic polylactide	11,800		[118]
Isotactic polylactide	4100		[118]
Ultra-high molecular weight polypropylene	6300		[99]
Atactic polypropylene	4390–7050		[13,15,112,119,120]
Syndiotactic polypropylene	1700–3400		[13,112]
Isotactic polypropylene	5500–9900		[13,99,106,111,112]
Atactic poly(methyl methacrylate)	10,000–13,600	29,500	[15,112]
Syndiotactic poly(methyl methacrylate)	5800–9200		[97,112]
Isotactic poly(methyl methacrylate)	14,600		[97]
Syndiotactic polystyrene	14,500		[121]
Isotactic polystyrene	17,500–28,880		[15,97,112,121]
Polycarbonate	1330–1660		[112,119]
Poly(ethylene terephtalate)	1170–1450		[15,97,119]
Poly(methylene oxide)	2110–2640		[15,97,119]
Poly(ethylene-2,5-furanoate)	3500		[122]
1,4- polybutadiene	1850		[123]
Poly(phenylene oxide)	3150–3620		[97,119]
Poly(tetrafluoroethylene)	5580		[97]
Poly(vinylidene fluoride)	2400		[97]
Poly(methyl acrylate)	9070		[97]
Poly(vinyl acetate)	9100–11,400	24,500	[15,97]
Poly(caprolactam)	2490		[97]
Poly(dimethylsiloxane)	8160–12,000	24,500	[15,97]
Atactic poly(1-hexene)	12,100		[124]
Syndiotactic poly(1-hexene)	14,100		[124]
Isotactic poly(1-hexene)	15,200		[124]
Atactic polystyrene	13,400–18,700	38,000	[15,97,112,113,121,125]

Methods for determining M_e using Equation (1) or Equation (5) are also applied to characterize partially disentangled polymers in the melt state. The correctness of such application may be a matter of debate, but so far there are no arguments against it.

3.2. Entanglements in Polymer Blends

Table 1 shows data characterizing the entanglements of homopolymers. However, entanglements also occur in blends of two or more polymers. The entanglement in the blend can be determined using rheological methods. In immiscible blends, it is assumed that the degree of entanglement is the same as in the polymers used. In the miscible blend, entanglement depends on the composition and the entanglement density of each blend component [126–128]. It has been observed that chemically dissimilar chains entangle more than similar chains, so their contribution to the total number of entanglements is large [126,129]. The contribution of different types of entanglements to the average

entanglement density in a blend ν_e, or to the average molecular mass between entanglement in a blend M_e has the form:

$$\nu_e = \frac{\rho}{M_e} = \frac{\varphi_1^2 \rho_1}{M_{e1}} + \frac{\varphi_2^2 \rho_2}{M_{e2}} + \frac{2\varphi_1\varphi_2\rho_1\rho_2}{M_{e12}} \tag{10}$$

where ρ is the density of the blend, ρ_1 and ρ_2 are the densities of the blend components, φ_1 and φ_2 are the volume fractions of the components, M_{e1} and M_{e2} are the molecular masses between the entanglements of the same polymer, and M_{e12} is the molecular mass between the entanglements of macromolecules of two polymers [129].

The rheology of compatible blends of poly(methyl methacrylate)(PMMA) and poly (styrene-acrylonitrile)(SAN) was investigated by Wu [130]. The G_N^0 modulus for the blend with 60–90% SAN was lower than the moduli of both components, which means that $M_{e12} > M_{e1}$ and $M_{e12} > M_{e2}$ (Figure 5a). An explanation has been proposed that the specific interchain interaction of dissimilar polymers tends to locally align the chain segments, stiffening the chains, and reducing the convolution, resulting in reduced entanglement between dissimilar chains. Other blends studied by Wu [131] were PMMA/poly (ethylene oxide), PMMA/poly(vinylidene fluoride), and polystyrene/poly(phenylene oxide). For these blends, the G_N^0 modulus was always between the values for the pure blend components, although a negative deviation from the straight line was visible.
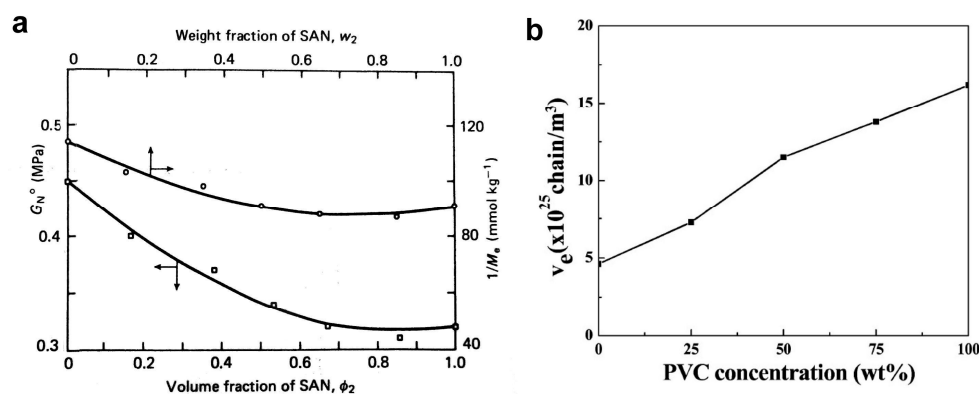

Figure 5. (**a**) Plateau modulus G_N^0 as a function of the volume fraction φ_2 of SAN in the PMMA blend, and $1/M_e$ versus weight fraction w_2 of SAN. The arrows on the curves show their corresponding axes. Reproduced with permission from ref. [130]. Copyright 1987. Elsevier. (**b**) Entanglement density, ν_e, as a function of PVC content in PVC/α-MSAN blends. Reproduced with permission from ref. [126]. Copyright 2013. American Chemical Society.

An example of the multicomponent blends studied was that described by Song et al. [126]. They analyzed miscible blends of poly(vinyl chloride) (PVC)/poly (α-methylstyrene-acrylonitrile) (α-MSAN) toughened with polybutadiene-g-poly(styrene-co-acrylonitrile)(PB-g-SAN). The entanglement density as a function of PVC content was calculated according to Equation (1), based on the results of rheological measurements of G'. An approximately linear relationship was found (Figure 5b).

Song et al. [132] also examined miscible blends of polyphenylene oxide/polystyrene (PPO/PS) toughened by high-impact polystyrene (HIPS) and polybutadiene-graft-polystyrene (PB-g-PS) copolymer. The authors assumed that the blends had an equilibrium density of entanglements, proportional to the composition. It was observed that mechanical properties, i.e., impact strength and elongation at break, gradually increased with the assumed entanglement density of the matrix.

The properties of UHMWPE were modified by blending with PP [133]. A significant reduction in the apparent melt viscosity was observed, and for the blend with 20% of PP, the entanglement density, ν_e, determined from the storage modulus on the rubbery plateau,

was 181 mol/m^3, i.e., lower than that of UHMWPE, which was 433 mol/m^3. Adding 1 wt.% poly(ethylene glycol) to the UHMWPE/PP blend further reduced ν_e to 147 mol/m^3.

3.3. Partially Disentangled Melts

The development of methods for disentangling macromolecules has opened the possibility of deeper exploration of the role of entanglements. Studies usually involve the comparison of entangled and partially disentangled polymers. The frequency sweep test is often performed using a rotational rheometer to demonstrate the change in G′ and G″ moduli and the change in complex viscosity. Figure 6a illustrates the change in complex viscosity as a function of frequency, measured for the same polypropylene, but disentangled to different extents [106]. PPNi is a fully entangled polymer with M_e = 9900 g/mol, and PPN0.5 is the most disentangled polymer with M_e = 19,100 g/mol. The decrease in viscosity values with disentanglement is visible, as is the reduction in G′ at high frequencies (Figure 6b) in measurements of differently entangled polylactide (PLA) [117].
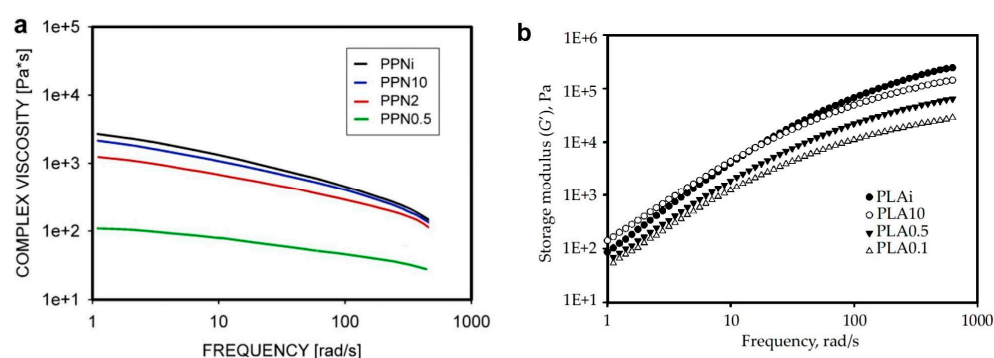

Figure 6. (**a**) Complex viscosity of polypropylene as a function of frequency and disentangling. PPNi –fully entangled polypropylene with M_e = 9900 g/mol, PPNi10—polypropylene with M_e = 12,600 g/mol, PPN2—polypropylene with M_e = 18,000 g/mol, PPN0.5—polypropylene with M_e = 19,100 g/mol. Reproduced with permission from ref. [106]. Copyright 2019. Elsevier; (**b**) Storage modulus G′ as a function of frequency, measured at 180 °C. PLAi –fully entangled polymer with M_e = 10,500 g/mol, PLA10—partially disentangled PLA with M_e = 16,300 g/mol, PLA0.5—PLA with M_e = 32,800 g/mol, PLA0.1—PLA with M_e = 65,300 g/mol. Reproduced with permission from ref. [117]. Copyright 2020 by Lukasiewicz Research Network—Industrial Chemistry Institute.

A decrease in the plateau modulus was found when metallocene-catalyzed high-density polyethylenes (HDPEs) were compared with commercially available HDPE [114]. This was due to a reduction of entanglements during metallocene-catalyzed polymerization. The effect of polymerization conditions on the entanglement of ultra-high molecular weight polyethylene (UHMWPE) was studied using rheological amplitude sweep and time sweep tests by Pandey et al. [23] and Chen et al. [134]. The conclusion was that slower polymerization led to fewer entanglements per unit chain length. When UHMWPE polymerization was carried out in the presence of polyhedral silsesquioxane (POSS), more entanglements in the polymer were obtained because POSS limited crystallization and created conditions for entanglement of growing chains instead of their participation in crystallization [135].

Drakopoulos et al. [136] studied the relaxation dynamics of UHMWPE using torsional rheology and observed different γ-relaxation behavior of disentangled and entangled polymer, suggesting that the entanglement density affects the free volume and thus affects the γ-relaxation. The analysis of the dynamic viscosity of cereal starches was conducted by Guo et al. [137,138]. The samples were prepared from aqueous solutions with concentrations above or below the critical concentration, which was determined based on measurements of the change in the slope of specific viscosity as a function of concentration. This critical concentration varied significantly (3.3–16.9%, g/L), depending on the type of starch. The cross-over frequency was used to characterize the starch rheology, except for the samples

prepared from 1 wt.% solutions, for which no cross-over point was observed, which was explained by the very low density of interchain entanglement in these samples.

The subject of studies in the last decade has also been the rheology of nanocomposites [139–143]. Several authors observed that when nanoparticles were well dispersed in the polymer matrix, the melt viscosity of the system was reduced, unlike composites with micro-sized fillers or nanofiller agglomerates, in which the viscosity increased [142,144]. The effect of viscosity reduction depends on the size of the nanoparticle, which should be smaller than the mesh size of the matrix [140]. Sufficiently small particles can increase the free volume of the melt, thereby reducing chain entanglement and accelerating the relaxation of the molten matrix. Examples of nanocomposites whose rheology was studied were poly(methyl methacrylate)-silicon [142], polystyrene–polyoxymetalate [140], UHMWPE-POSS [144], UHMWPE-TiO_2 [145].

3.4. Re-Entangling of Polymers

Many of the disentangled polymers were studied using a rheological time sweep test. The goal was to show how moduli and viscosity change over time [43,106,135,146–151]. This experimental interest resulted from the expectation that after a sufficiently long time at high temperature, the macromolecules would re-entangle, i.e., the polymer would be in equilibrium again and the rheological parameters would reach their initial values (Figure 7a). Research has shown that this does not often occur within a reasonable experimental time. Many authors treated achieving a constant value of the G' modulus as a criterion for reaching the equilibrium entangled state, even if the value of this modulus was lower than initially. The results were then presented in normalized form, i.e., as the ratio of the actual G' value to the constant G' value at the end of the test (Figure 7b).

Regardless of the definition used, the time after which the disentangled polymer reached constant values of rheological parameters was long and depended on the molecular weight of the polymer. For example, for linear polyethylene, it increased from 100 s to 11 h when the molecular weight increased from 9.0×10^4 to 3.6×10^6 g/mol [152]. Even longer times, e.g., 55–118 h, were measured for UHMWPE with $M_w = 5 \times 10^6$ g/mol [23,153] (Figure 7c). The proposed explanation for the long times observed is that as the molecular weight increases, the number of entanglements per chain also increases, so it takes longer to reach a thermodynamically stable state. Talebi [60] found that the relationship between the time of re-entangling of UHMWPE, t, and its molecular weight M_w is:

$$\ln t = a \times 2.8 (\ln M_w) \tag{11}$$

where a is a constant.

The influence of polymerization conditions, and therefore disentanglement, on rheological properties were observed by Rastogi et al. [154], Chen et al. [134], and Ronca et al. [43]. The reduction of entanglement time resulting from melt annealing of UHMWPE was found by Li et al. [104]. The reason was the increased chain mobility at high temperatures. The dependence of the entanglement time on the density of entanglements was not confirmed in the study of two UHMWPEs by Chammingkwan et al. [48]. However, careful analysis showed that the most likely cause was the presence of voids in the entangled polymer, which reduced contact of the polymer with the rheometer plates.

Sometimes, during time sweep experiments, it is observed that the increase in modulus is not smooth, but undulations, i.e., periodic fluctuations, are visible (see Figure 7a) [37,147,149]. The reasons for this phenomenon have not yet been explained and it cannot be ruled out that there are technical, instrumental causes of measurement disturbances.
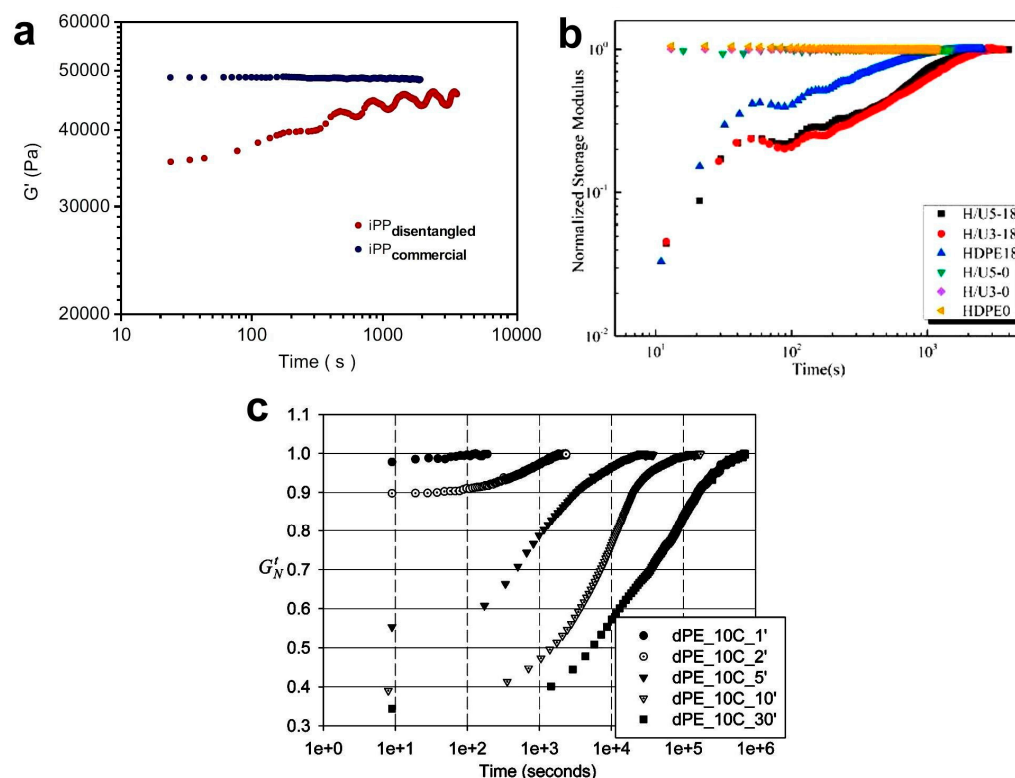
Figure 7. (**a**) Changes in the G′ modulus as a function of time, measured at 180 °C on entangled and disentangled PP. Reproduced with permission from ref. [37]. Copyright 2009. Elsevier. (**b**) Buildup of normalized storage modulus for HDPE/UHMWPE blends at 200 °C. The H/U5-18 designation means HDPE with 5% added UHMWPE sheared at rate of 18 s^{-1}. Reproduced with permission from ref. [149]. Copyright 2020. Elsevier. (**c**) Results of dynamic time sweep test performed at 160 °C for five UHMWPEs synthesized at low temperature with different polymerization times (1′–30′), leading to different entanglements. G′$_N$ is the elastic modulus normalized by maximum plateau modulus in the modulus buildup. Reproduced with permission from ref. [23] Copyright 2011. American Chemical Society.

Based on the shape of the G′ curves (Figure 7c), Pandey et al. [23] suggested that the re-entanglement process consists of two stages, with a rapid increase in G′ modulus and entanglements in the first phase and much slower entanglement in the second phase. For a semicrystalline polymer, Li et al. [135] associated the first phase with the process of explosive disintegration of crystals, analogous to the observations of the melting of single-crystal polyethylene mats carried out by Barham and Sadler [75]. The second phase of re-entanglement should be controlled by the reptation movement of the macromolecule chains. Similar explanations were also proposed by Pandey et al. [23] and Talebi [60]. A serious objection to this interpretation is the fact that the time of the first phase in the case of polyethylene is, according to the publication by Li et al. [135], as long as 6 h (see the dPE_10C_5′ curve in Figure 7c), which is much longer than usual crystal melting time. Rather, it appears that the melting of the crystals introduces a less entangled phase of the melt into the interior of the also partially disentangled melt derived from the amorphous phase. The equalization of the entanglement density, faster in the less entangled phase and slower in the more entangled phase, may be the cause of the macroscopically observed changes in moduli. Two stages of re-entanglement were also observed by Fu et al. [147]. In their opinion, these two stages differ in the type of entanglements that arise. In the initial phase (approximately 100 s for HDPE), simple entanglements (twists, knots, links) are formed, while in the second phase, loops are formed.

The time sweep test was used to investigate poly(L-lactide) re-entanglement. The polymer was disentangled by freeze-extraction from solutions of various concentrations [19].

The G′ modulus was lower for polylactide obtained from a less concentrated solution, which was consistent with expectations regarding the level of disentanglement. The time to reach equilibrium value G′ was longer for the less entangled polymer.

Another polymer for which entanglement restoration was studied was polystyrene [18]. Depending on the solution from which the polystyrene was obtained, starting from low concentrations, the re-entanglement time first decreased, while for higher concentrations the trend was opposite, i.e., the re-entanglement time increased (Figure 8). The behavior observed below a concentration of 3.0 in Figure 8 was as expected because more separated chains needed more time to entangle. For the high-concentration region, the explanation has been proposed that a more concentrated solution results in a smaller chain coil size and more compact globules after freeze-drying. Therefore, it takes more time for the coils to envelop the neighbors.
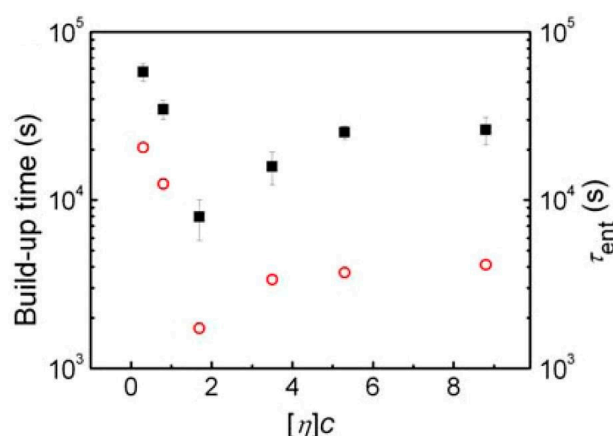

Figure 8. Equilibrium entanglement time of PS samples freeze-dried from solutions with different initial concentrations. The filled black squares refer to the modulus buildup time at which $G'(t)/G_N^0 = 0.98$, and the open red circles represent the calculated times of the entanglement recovery. Reproduced with permission from ref. [18]. Copyright 2012. American Chemical Society.

The re-entanglement has also been examined for PP [106]. It was found that after 2 h of melt annealing, the viscosity of PP still remained below the initial level, although during this time the mechanical properties typical for entangled PP were restored. It was observed that the re-entanglement time depended on the initial degree of entanglement, i.e., it was longer for the less entangled polymer, as well as on the molecular weight of PP. At larger M_w, re-entanglement required a longer time.

The rare case is the study of composites in which the polymer has reduced entanglement. An example is UHMWPE containing POSS nanoparticles introduced in various concentrations during polymerization [135]. The change in G′ over time is shown in Figure 9a, and the same data after normalization in Figure 9b. The highest initial storage modulus was found for a POSS content of 0.74%, and it decreased at higher POSS content. This was explained as a result of the highest molecular weight of this UHMWPE, which was polymerized with low filler content. Similarly to UHMWPE, the re-entanglement process in the UHMWPE/POSS nanocomposite required an extremely long time, exceeding 1000 min.

The partially disentangled PP composites with graphene nanoplatelets (0.1–4 wt.%) were prepared by the melt shear, and changes in the rheological properties of the melt were observed with time [155]. It was measured that partially disentangled neat PP tested at 200 °C needed 2000 s to reach the viscosity of fully entangled PP. Much shorter times of only 100 s were measured for the composites, however their final viscosities were at a lower level than for the entangled PP. The authors presented the opinion that the disentangled state remained at the observed level because the nanoplatelets, due to their strong interaction,

limited the movement of the chains. Doubts regarding the given explanation are raised by the fact that a similar effect was observed for some homopolymers.
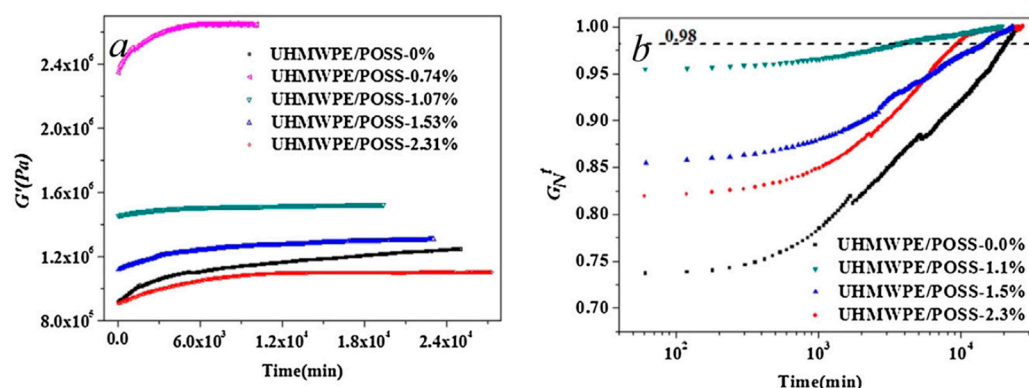

Figure 9. (**a**) Results of a dynamic time sweep test performed at 170 °C for UHMWPE with different POSS content. (**b**) Data from Figure 9a shown after normalization. G_N^f is the storage modulus normalized by the maximum recorded value. Reproduced with permission from ref. [135]. Copyright 2014. Elsevier.

Luo et al. [156] studied the re-entanglement of chains in a PP micro-composite with a high content (35 wt.%) of boron nitride. The disentanglement of the composite was achieved by steady-state shear. As expected, before shear was applied, the composite had a higher viscosity than PP. After shearing, the viscosity of the composite decreased below the PP level, but increased rapidly within the first 30 s after shear cessation and then remained stable at a level below the PP viscosity.

The build-up of entanglement as a function of time can also be characterized by measuring the normal force in the time sweep test performed with the rotational rheometer [19,60]. In the case of completely entangled UHMWPE, no changes in normal force were recorded, while in the case of disentangled polymer, a gradual decrease in normal force was observed over time. This was caused by a reduction in the free volume of the melt during the formation of entanglements.

The time sweep rheological test is most often used to characterize changes in entanglements with polymer residence time in the melt, but they can also be investigated using other rheological tests. For example, a strain sweep test and a frequency sweep test with multiple repeated cycles were used to characterize UHMWPE [104].

4. Mechanical Properties Dependent on the Entanglement of Macromolecules

4.1. Properties of Equilibrium Entangled Polymers

The presence of entanglements in an amorphous polymer or in the amorphous phase of a semi-crystalline polymer determines the mechanical properties of the entire polymer [157]. In both amorphous and semicrystalline polymers, the main deformation features, mainly examined in the tensile test, are the same. Under the action of force, the deformation is initially elastic, followed by yielding when segmental rearrangements are possible. With a larger deformation, strain softening may occur, resulting from localized plastic deformation leading to necking. The strain softening is usually not visible when results are presented as a true stress–true strain curve. As the strain increases, plastic flow is observed at an approximately constant stress level, followed by an increase in stress, which is known as strain hardening [158]. Based on the behavior of deformed polystyrene and polycarbonate, it can be shown that the strain hardening is more pronounced when the polymer is more entangled [159]. At large deformations, orientation and stretching of macromolecules with their partial disentanglement are observed [160].

The deformation phases described above are observed when the polymer is ductile, and only some of them when the polymer is brittle. The same polymer can become brittle or ductile depending on the temperature and the strain rate. The irreversible plastic

deformation of amorphous polymers occurs through the formation of shear bands or crazes. Essentially the same deformation phases are visible when the polymer is compressed [158] (Figure 10).
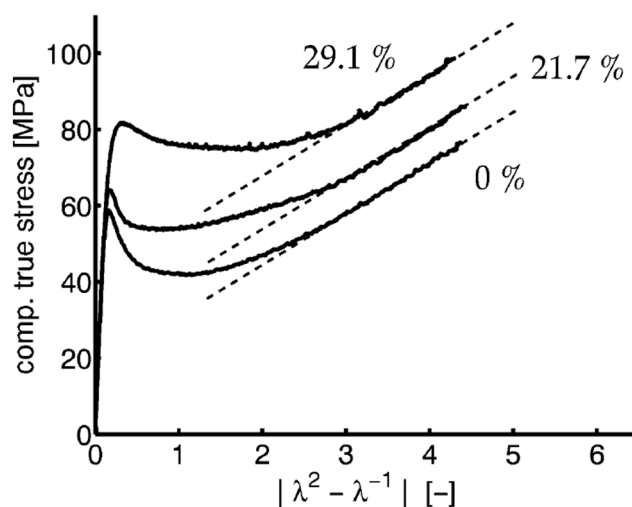

Figure 10. Compressive behavior of isothermally crystallized poly(ethylene terephthalate) samples with different degrees of crystallinity. λ is the extension ratio. Reproduced with permission from ref. [158]. Copyright 2004. American Chemical Society.

The deformation of a semicrystalline polymer analyzed at the micro-scale is more complicated because its structure contains crystalline lamellae connected by macromolecules [4]. The two main types of connections are tie macromolecules, that is, macromolecules having fragments in neighboring crystals, and macromolecular entanglements [160]. Therefore, in semicrystalline polymers, the physical cross-links of the macromolecular network are both the entanglements in the amorphous phase and the crystals themselves [4]. The main stages of the evolution of the semicrystalline polymer structure in relation to the strain–stress dependence were described by Strobl [4,161–163]. At small strains (point A in Figure 11) single acts of deformation occur in the form of lamellar separation, rotation of lamellae, and interlamellar slips. At the yield point (B), massive chain slips are initiated. The amorphous chains gradually orient with increasing deformation. During the strain softening (C), lamellar fragmentation occurs, and fibrillation begins, i.e., the formation of fibrils by fragmented, oriented crystallites. Once a plateau is reached (point D), the chains begin to disentangle, allowing further deformation, with the neck propagation through the sample. At larger strains, the strain-hardening begins due to the stretching of the macromolecular network (E).

Men et al. [166] studied the deformation at point C. They changed the density of entanglements of selected polymers by blending them with other miscible polymers and analyzed the free shrinkage of these materials. It was found that stretching a semicrystalline polymer always results in the deformation of the interpenetrating networks of interlocked crystallites and the entangled amorphous phase. The deformation from point B is dominated by the stretching of the amorphous phase, controlled by entanglements.

Although entanglements are involved in all phases of deformation, attention is focused on the strain-hardening phase, when changes in the entropy of the entangled network occur, resulting from its stretching, orientation, and possible partial disentangling.
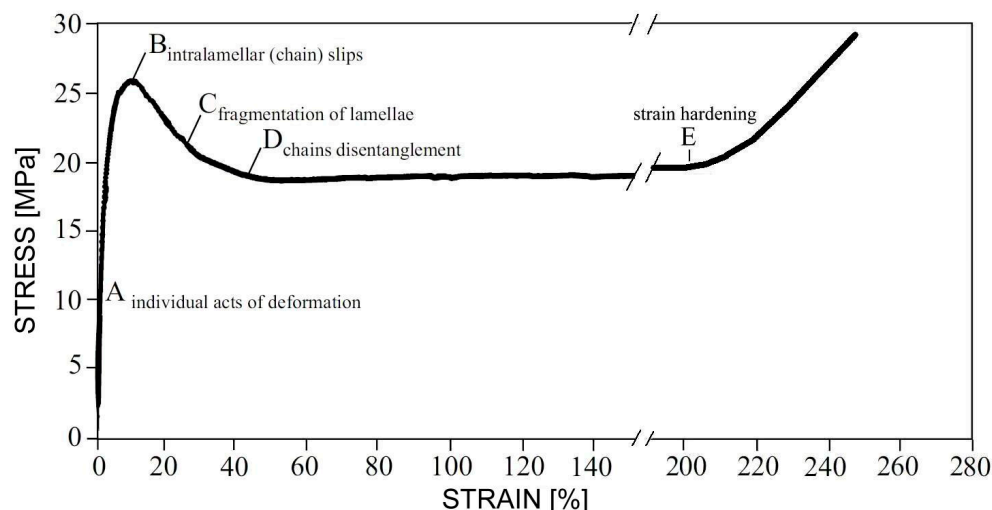
Figure 11. The stress–strain relationship for high-density polyethylene deformed in tension. The characteristic deformation points are marked A–E. Previously published experimental data [164,165] were used to prepare the figure.

The plastic phase of deformation during polymer stretching can be described by an equation of the form [167]:

$$\sigma = \sigma_y + \lambda(NkTn^{0.5})/3\,[\lambda(3 - \lambda^2/n)/(1 - \lambda^2/n) - 1/\lambda^2(3 - 1/\lambda n)(1 - 1/\lambda n)] \tag{12}$$

where σ is the true stress, σ_y is the yield stress, N is the number of entanglements per unit volume, n is the number of flexible units between entanglements, and λ is the extension ratio. When n is large or λ is small, the Equation (11) can be simplified and takes the form [168,169]:

$$\sigma(\lambda) = \sigma_y + G_R(\lambda^2 - 1/\lambda) \tag{13}$$

where G_R is the strain-hardening modulus. G_R depends on the temperature T and the entanglement density ν_e [128,170]:

$$G_R \sim \nu_e/T \tag{14}$$

According to this equation, the slope of the strain-hardening phase, as proportional to the physical cross-links, should increase with the entanglement density [158]. Equations (12)–(14) do not contain M, therefore it is assumed that the strain-hardening and the entanglement density should be independent of the molecular weight. However, in the case of semi-crystalline polymers, due to the presence of a crystalline phase, tensile and compression properties suggest that there is an influence of molecular weight [158]. The reasons for this are discussed later in the text.

There is one more parameter characterizing the polymer network that depends on entanglements. This is the maximum draw ratio, related to the square root of M_e [171,172]. The entanglement network affects not only the shape of the stress–strain relationship but also the micro-mechanisms of deformation, such as crazing and/or shear yielding [173–175]. This issue is especially important for amorphous polymers.

The relationships presented above (Equations (12)–(14)) result from both theoretical and experimental research [158,176,177]. The experiments confirmed that the strain hardening occurs earlier and is stronger when the density of entanglements is higher. Figure 12 shows the strain–stress relationship for a series of polyethylenes with different molecular weights [176]. The authors explained changes in the strain-hardening slope with a change in M_w as the result of an increase in the entanglement density with an increase in molecular weight. For the same reasons, a decreased deformation ratio was observed.
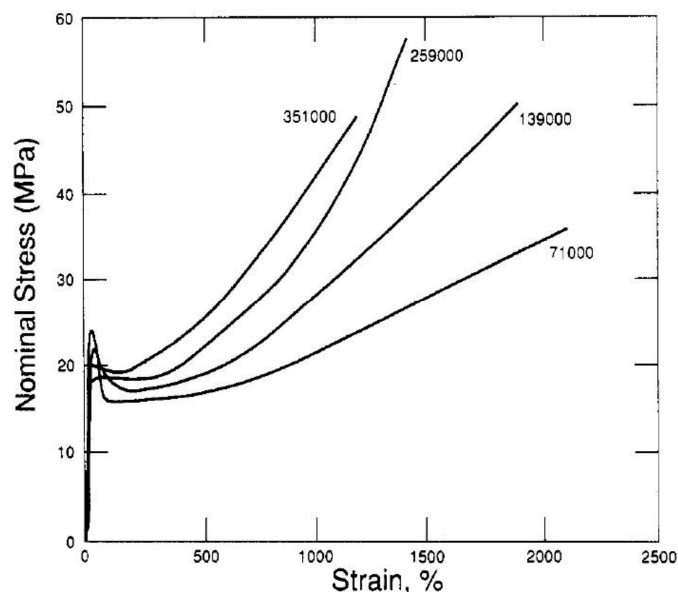
Figure 12. Nominal stress versus nominal strain for a series of rapidly quenched linear polyethylenes with the most probable molecular weight distributions (see numbers on curves). The strain hardening phase is clearly visible, earlier for higher molecular weight. Reproduced with permission from ref. [176]. Copyright 1994. American Chemical Society.

Schrauwen et al. [158] examined the properties of polyethylene, polypropylene, and poly(ethylene terephthalate) during uniaxial compression. One of their conclusions was that the strain-hardening depended on the sample preparation, i.e., slowly crystallized samples exhibited lower strain-hardening. According to the authors, this was due to the lower density of chains in the amorphous phase, resulting from the pulling out of the macromolecular chains during slow crystallization. The similarity of results for different polymers supported the opinion that the crystalline phase does not contribute to strain-hardening, which is controlled by the chain entanglement density. Schrauwen et al. [158] agreed with Kenendy's [176] opinion on the influence of M_w on the chain entanglement density, explaining that the more difficult pulling out of chains during the crystallization of polymer with higher M_w.

Polyethylenes with M_w in the range of 5×10^4 to 5×10^6 g/mol were examined by Bartczak and Kozanecki [177]. The experimental stress–strain curves were fitted using the Arruda and Boyce model [178]. The authors obtained a decrease in M_e from 1020 to 414 g/mol as M_w increased. The reason for the change in M_e was differences in the structure of the amorphous phase, resulting from a different course of crystallization. According to the authors, during the plastic deformation, partial disentangling of polymer chains occurs.

4.2. Properties of Disentangled Polymers

In the above-described experiments, the differences in entanglements resulted from the crystallization conditions, but in the 1970s it was already possible to study polymers disentangled in solutions. The influence of entanglement reduction on mechanical properties was found when Lemstra and Smith [179] performed experiments involving the spinning of polymer solutions after gelation. They observed that polyethylene gel could be spun to very high ratios (about 30 times) and create strong fibers with an elastic modulus of 108 GPa [179,180]. The reason for the excellent drawability of polyethylene was the reduction of entanglements in the gel [29].

Smith and Lemstra also made a film by drying a UHMWPE gel and found that very high strains could be achieved, while the same polymer processed by melting showed much earlier breaking [179] (see Figure 13). The ultradrawing behavior of gel films was also studied by Yeh et al. [181]. A high deformation ratio of 60 was obtained for a film made of ultra-high molecular weight polypropylene (UHMWPP) prepared from a gel

solution [38]. Similarly prepared UHMWPP sheets were subject to a two-step drawing by Ikeda et al. [182]. The samples for the second stage were cut from the sheets pre-drawn in the first stage. The tensile drawing of samples to break was performed at high temperatures of 130 °C or 150 °C. Based on the determined draw ratio of the neck and the maximum draw ratio of the sample, the authors concluded that both depend on the inverse root of the concentration of the solution from which the sheet was cast.
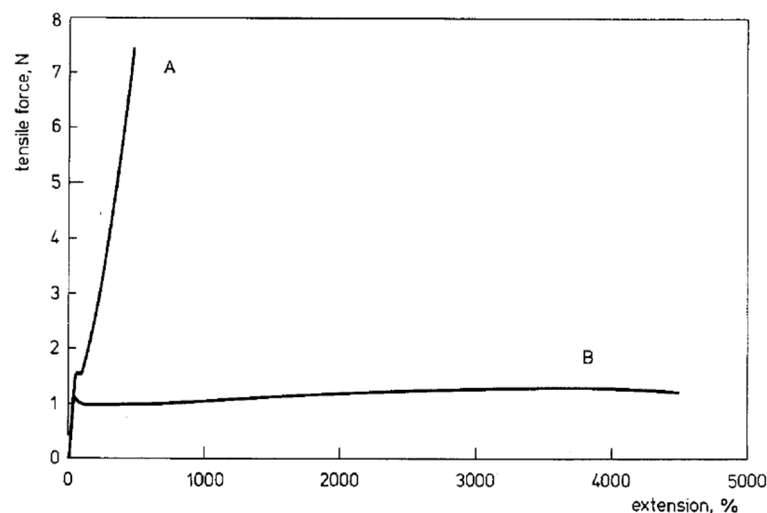

Figure 13. Load–extension curves measured at 120 °C for UHMWPE. A—melt crystallized film, B—film cast from 2 wt.% solution in decalin, with reduced entanglements. Reproduced with permission from ref. [179]. Copyright 1980. Springer Nature.

One of the earlier works using the freeze-drying disentangling method was the one published by Huang et al. [183], in which poly(ethylene terephthalate) obtained from the solutions with a concentration of 2–40 wt.% was drawn by solid-state co-extrusion at the temperature of 70 °C. The maximum extrusion draw ratio achieved depended on the concentration of the solution from which the polymer was obtained. At very low concentrations the density of entanglement was too low to ensure the continuity of the material, while at too high concentrations the entangled network prevented high drawability.

Studies of the tensile deformation of entangled and partially disentangled polypropylenes obtained by crystallization from solutions at temperatures 20–100 °C were carried out by Pawlak et al. [184]. The measured masses between entanglements were 9.9, 14.5, and 18.0 kg/mol. Mechanical properties before and at the yield did not change due to the reduction of entanglements, but the strain-hardening increased with the density of the molecular network formed by entanglements (Figure 14a). It is known that semi-crystalline polypropylene cavitates during tensile deformation [185]. However, for the first time in the case of polymers, it was observed that the reduction of entanglements intensifies cavitation (Figure 14b). The cavitation in disentangled polypropylene was possible not only at low temperatures, as is usually the case, but even when the tensile test was performed at the temperature of 100 °C.

The process of void generation during uniaxial stretching was modeled using the molecular dynamics method by Logunov and Orekhov [186]. They modeled the properties of amorphous polyethylene and concluded that the molecular entanglements slow down the growth of voids and their aggregation in the bulk of polyethylene.
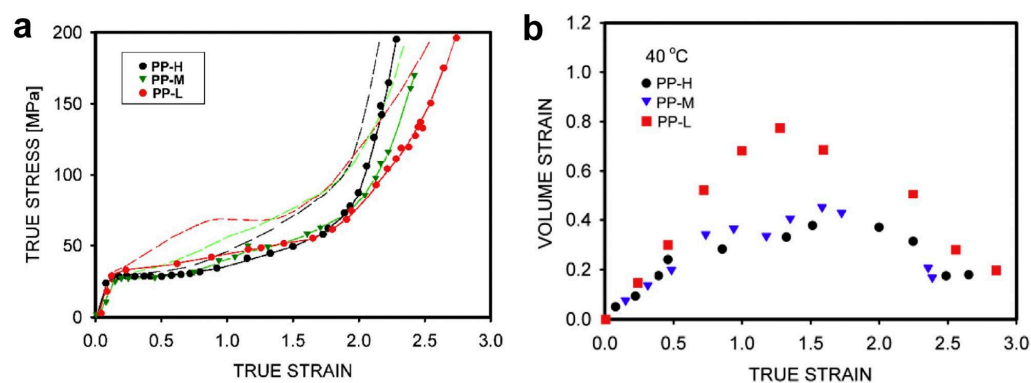
Figure 14. (**a**) True stress–true strain curves for polypropylenes deformed at 40 °C. PP-H is entangled polymer with M_e = 9.9 kg/mol, and PP-M and PP-L are partially disentangled polypropylenes with M_e = 14.5 kg/mol and M_e = 18.0 kg/mol, respectively. The strain-hardening, dependent on entanglement, is visible from the true strain of 1.9. The dashed lines show the shapes of curves after correction of the cross-section area and the strain for the presence of voids fraction in bulk samples; (**b**) The evolution of volume strain during deformation. The volume strain is a measure of the increase in sample volume due to the cavitation. Reproduced with permission from ref. [184]. Copyright 2018. Elsevier.

The tensile properties of polycarbonate disentangled to varying degrees by using modified shear procedures during extrusion (by rotation, vibration, or together), were examined by Wang et al. [55]. Although the decrease in viscosity was confirmed rheologically, the most disentangled sample had tensile properties similar to those made from raw pellets. The reason for this was not discussed. The authors presented some conclusions regarding processability using the injection molding method. The lower processing temperature and pressure when the polymer was disentangled were beneficial for molding the products, obtaining lower residual stresses and therefore better (slightly) mechanical properties. The disentangled sample, having a reduced melt density, can be expected to show superiority over the original material when it becomes difficult to fill the mold during injection molding.

If the mechanical behavior in the strain-hardening phase depends on M_e, a change in slope should be visible when the initially disentangled polymer is re-entangled by melt annealing. The solution-disentangled PP samples were annealed at different times and examined in a compression test by Krajenta et al. [106]. The choice of compression rather than extension was intended to avoid the potential impact of cavitation. Figure 15 shows that the stress–strain curves of the entangled sample and the annealed sample overlap after 2 h when the PP has M_w = 250 kg/mol, but 2 h of annealing was not sufficient for fully re-entangle the polymer with higher M_w = 400 kg/mol.

Although tensile testing is most commonly used to characterize mechanical properties, studies on impact behavior have also been performed. The Izod impact test was used to measure the strength of two sintered UHMWPEs, fully entangled and partially disentangled [187]. This less entangled polyethylene showed an impact strength of 80 kJ/m^2, while the entangled PE showed an impact strength of only 70 kJ/m^2. The unexpected result was probably due to better sintering of the grains in the sample with more mobile macromolecules.

In the UHWWPE research, Zhang et al. [188] used the Charpy version of the impact test. The commercial polymers used (SLL 5 and GUR 4150) had the same M_w, so the molecular weight should not affect the impact strength. Tensile testing, a prelude to the main tests, showed stronger strain-hardening for SLL 5, which indicated more entanglements. This was also confirmed by rheology. In the impact measurements, the less entangled polyethylene had three times higher Charpy impact strength than the entangled polyethylene (144 kJ/m^2 vs. 43 kJ/m^2). The GUR 4110 sample showed a ductile fracture, while the SLL 5 samples fractured brittle. The authors interpreted the observed differences as related to the different

structures of polymers, i.e., smaller nascent particles and a lower degree of entanglement, which led to a better connection of the polymer grains during film formation.
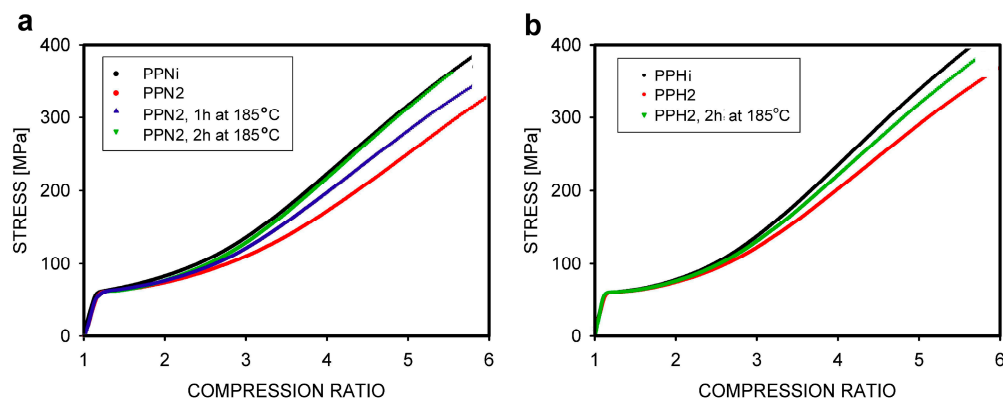

Figure 15. Mechanical properties of compressed polypropylenes with different entanglement densities: (**a**) PPNi—initial polypropylene with M_w = 250 kg/mol, PPN2 –the same polymer after disentanglement, non-annealed and annealed 1 h or 2 h; (**b**) PPHi—initial polypropylene with M_w = 400 kg/mol, PPH2 –the same polymer after disentanglement, non-annealed and annealed 2 h. Reproduced with permission from ref. [106]. Copyright 2019. Elsevier.

Other impact properties were tested on micro-sized spherical polystyrene projectiles [125]. The projectiles had different M_w in the range of 9.3–270.0 kg/mol, so one of them had a value below M_e = 13.4 kg/mol. The spheres were launched against a rigid substrate, which led to deformation at an ultra-high strain rate. During impact, the bottom of the projectile heated up and deformed in plastic flow. In the upper part, a localized shear banding with brittle fracture was observed for spheres from disentangled PS and extensive shear banding followed by crazing in the entangled projectiles. The absence of entanglements resulted in a rapid transition to fracture.

One way to improve the processability of UHMWPE, which is unsatisfactory due to $M_w > 10^6$ g/mol, is to blend it with lower molecular weight polyethylene, which is the main component of the formed blend. Compatible high-density polyethylene (HDPE) or linear low-density polyethylene (LLDPE) macromolecules penetrate UHMWPE during blending, reducing its entanglements [189,190]. Chen et al. [191] prepared blends of HDPE with disentangled or entangled UHMWPE obtained directly in the reactor. With the same composition, the tensile properties, such as elastic modulus, elongation to break, and tensile strength, of the blends with the entangled and disentangled components were similar (Figure 16). The big difference was in the impact strength, where the partially disentangled samples showed 2–3 times more energy absorbed at the break. The reason was a change in the internal structure. Disentangling the chains promoted more efficient growth of oriented shish-kebab structures, which were also longer in partially disentangled material.

Similar observations regarding the promotion by disentanglement of the growth of more oriented shish structures, with more densely attached kebab-like lamellae, were made by Tao et al. [192]. In their three-component polyethylene blend, weakly entangled UHMWPE macromolecules acted as tie molecules and significantly improved the impact resistance.

Although most studies of mechanical properties on reduced entanglements of macromolecules have been conducted using homopolymers, some studies have also been performed on polymer composites. The processability and tensile mechanical properties of UHMWPE were improved by adding 0.1–0.5 wt.% TiO_2 nanoparticles into the dilute UHMWPE solution [145]. The dispersion of nanoparticles changed with their concentration, from homogeneous through clusters to aggregates. The viscosity of composites with dispersed TiO_2 was lower than that of pure partially disentangled UHMWPE, reaching a minimum for content of 0.3 wt.% which meant a 50% decrease in entanglement. The presence of nanofiller increased the crystallinity by 7%, which together with the reduction in

entanglement, influenced the mechanical properties. Figure 17 shows the drastic difference in the tensile properties of the partially disentangled UHMWPE and its composite.
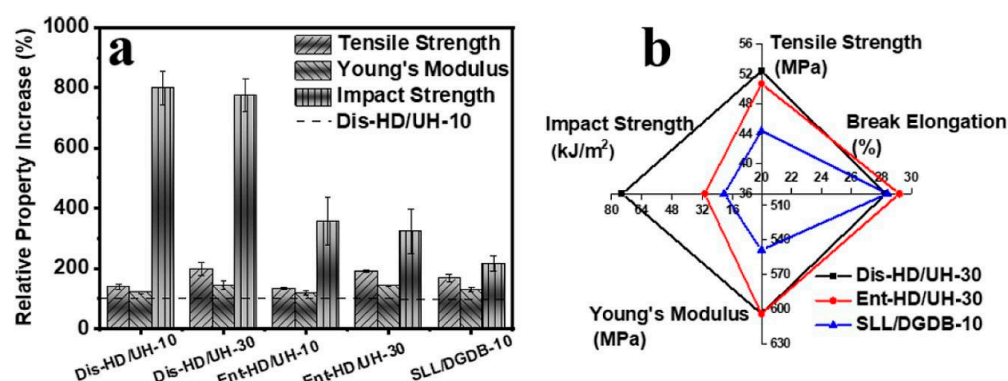

Figure 16. Comparison of the mechanical properties of synthesized HDPE/UHMWPE blends containing disentangled or entangled UHMWPE: (**a**) Improvement of the mechanical properties of blends in relation to the properties of HDPE, assumed as 100%. Dis-HD/UH-30 is the blend containing 30 wt.% disentangled UHMWPE, and Ent-HD/UH-30 is the blend containing 30 wt.% of entangled UHMWPE. Dis-HD/UH-10 is the blend containing 10 wt.% disentangled UHMWPE, and Ent-HD/UH-10 is the blend containing 10 wt.% of entangled UHMWPE. SLL/DGDB-10 is the commercial component blend containing 10 wt.% UHMWPE, shown for comparison. (**b**) Graphical presentation of the results for selected blends. Reproduced with permission from ref. [191]. Copyright 2023. American Chemical Society.
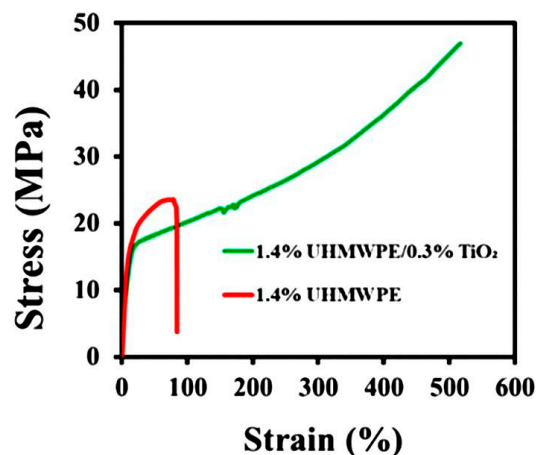

Figure 17. Tensile properties of UHMPE partially disentangled in a 1.4% wt. solution in decahydron-aphtalate and a similarly prepared UHMWPE/TiO$_2$ composite. Reproduced with permission from ref. [145]. Copyright 2023. Royal Society of Chemistry.

The properties of disentangled PLA and its composites containing 0.1–1 wt.% of multi-walled carbon nanotubes were investigated in comparison to entangled materials in the tensile test [193]. The test samples were prepared by extrusion. Better dispersion of the filler was obtained inside the less entangled polypropylene. During the deformation of the less entangled homopolymer, the initiation of plastic deformation occurred at a lower yield stress, and the stress increased more slowly during the strain-hardening. In the composite, the strain-hardening was stronger for the less entangled polylactide due to better dispersion of the filler.

Smith and Lemstra's [179] approach to forming fibers from a dilute solution, described above, was successful because the entanglement density in the polymer used was reduced. On this basis, Galeski developed the concept of producing all-polymer composites using the disentangled polymer to prepare fibers while mixing with a second polymer [194]. The

mixing takes place in the extruder at a temperature higher than the melting point of the polymer for matrix, but lower than the melting temperature of the disentangled polymer. When shear stresses are applied during mixing, the grains of the disentangled polymer are oriented and form fibers. At the end of mixing, when the temperature decreases, an all-polymer composite is obtained.

An example of the application of this concept was the preparation of a composite of ethylene–octene copolymer (EOC) and polypropylene with a composition of 96:4 wt.% [195]. Previously disentangled PP powders were used to prepare composites by extrusion. Microscopic observation confirmed that a network of PP fibers was formed inside the EOC during extrusion (Figure 18a). This resulted in increased stresses during tensile deformation compared to pure EOC (Figure 18b). The increase in stress was greater in the case of PP obtained from a more dilute solution, from which thinner fibers were formed, giving at the same content a larger contact area between components, and thus better reinforcing the composite matrix.
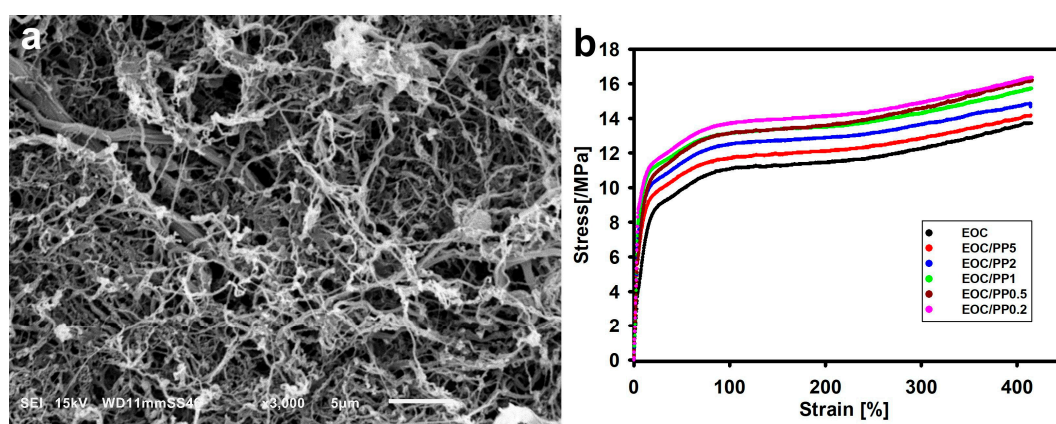

Figure 18. (**a**) Morphology of polypropylene fibers exposed after dissolving the EOC/PP composite in heptane. The fibers were formed from partially disentangled polypropylene, obtained from 0.2 wt.% solutions in xylene. (**b**) Tensile properties of EOC and composites with 4 wt.% of PP. The numbers in the description indicate the concentration of solution from which the partially disentangled PP was obtained. A lower number corresponds to a lower density of entanglements. Reproduced with permission from ref. [195]. Copyright 2024. John Wiley and Sons (Hoboken, NJ, USA).

5. Concluding Remarks

Until a few years ago, the disentangling of macromolecules was performed almost exclusively in the laboratory, and the goal was to better understand the impact of entanglements on the properties of polymers. Now that the entanglement-limited polymerization process has been mastered and it is possible to disentangle polymers during extrusion, we can think about the production of commercial polymers with limited entanglements, most likely useful in special applications.

From the point of view of processing and subsequent applications of the polymer, rheological and mechanical properties are particularly important. Rheological studies show that the disentangling of macromolecules leads to a decrease in the viscosity of polymer melt and a decrease in modulus values. The behavior of polymers at the micro level has already been quite well described by the tube model. One conclusion is that the time for the macromolecule to disentangle itself from the tube is quite long. This can be seen when performing experiments on the re-entanglement of macromolecules. However, polymer re-entanglement requires additional research, because existing descriptions of the phenomena raise doubts. It should be explained why there are two phases of the process and why the final modulus values are in many cases lower than expected. There is a lack of a more complete description of the rheological behavior of polymer blends and composites containing partially disentangled polymer. It has been reported that during

composite preparation, melt mixing of the disentangled polymer has a beneficial effect on the dispersion of the nanofiller.

The mechanical properties are as important as the rheological properties. There is a consensus that during the tensile test, usually performed, but also during the compression test, the presence of entangled macromolecules has the greatest impact on the strain-hardening phase of deformation. The stress buildup and strength of the tested polymer depend on the entanglement network. Few research results indicated a positive change in impact properties due to partial disentanglement of macromolecules. This seems to be due to the improved consistency of the tested material, obtained during the processing of a polymer characterized by increased macromolecular mobility. Research on mechanical properties has so far focused on homopolymers. Experiments are necessary to show how the properties of composites change, for example as a result of better dispersion of the reinforcement.

Author Contributions: A.P. and J.K. participated in collecting information and writing the text. All authors have read and agreed to the published version of the manuscript.

Institutional Review Board Statement: Not applicable.

Informed Consent Statement: Not applicable.

Data Availability Statement: No new data were created.

References

1. Everaers, R.; Sukumaran, S.K.; Grest, G.S.; Svaneborg, C.; Sivasubramanian, A.; Kremer, K. Rheology and microscopic topology of entangled polymeric liquids. *Science* **2004**, *303*, 823. [CrossRef]
2. Wool, R.P. Polymer entanglements. *Macromolecules* **1993**, *26*, 1564–1569. [CrossRef]
3. Berry, G.C.; Fox, T.G. The viscosity of polymers and their concentrated solutions. *Adv. Polym. Sci.* **1968**, *5*, 261–357.
4. Hiss, R.; Hobeika, S.; Lynn, C.; Strobl, G. Network stretching, slip processes, and fragmentation of crystallites during uniaxial drawing of polyethylene and related copolymers. A comparative study. *Macromolecules* **1999**, *32*, 4390–4403. [CrossRef]
5. Ferry, J.D. *Viscoelastic Properties of Polymers*, 3rd ed.; John Wiley & Sons: New York, NY, USA, 1980; p. 372.
6. Doi, M.; Edwards, S.F. *The Theory of Polymer Dynamics*; Clarendon: Oxford, UK, 1986.
7. Treloar, L.R.G. *The Physics of Rubber Elasticity*, 3rd ed.; Clarendon Press: Oxford, UK, 1975; pp. 64–65.
8. Ward, M.; Sweeney, J. *Mechanical Properties of Solid Polymers*; John Wiley & Sons Ltd.: Chichester, UK, 2013; p. 72.
9. Haward, R.N. Strain hardening of thermoplastics. *Macromolecules* **1993**, *26*, 5860–5869. [CrossRef]
10. Deplancke, T.; Lame, O.; Rousset, F.; Seguela, F.; Vigier, G. Mechanisms of Chain Reentanglement during the Sintering of UHMWPE Nascent Powder: Effect of Molecular Weight. *Macromolecules* **2015**, *48*, 5328–5338. [CrossRef]
11. Danielsen, S.P.O.; Beech, H.K.; Wang, S.; El-Zaatari, B.M.; Wang, X.; Sapir, L.; Ouchi, T.; Wang, Z.; Johnson, P.N.; Hu, Y.; et al. Molecular Characterization of Polymer Networks. *Chem. Rev.* **2021**, *121*, 5042–5092. [CrossRef]
12. Liu, C.; He, J.; van Ruymbeke, E.; Keunings, R.; Bailly, C. Evaluation of different methods for the determination of the plateau modulus and the entanglement molecular weight. *Polymer* **2006**, *47*, 4461–4479. [CrossRef]
13. Eckstein, A.; Suhm, J.; Friedrich, C.; Maier, R.; Sassmannshausen, J.; Bochmann, M.; Mulhaupt, R. Determination of Plateau Moduli and Entanglement Molecular Weights of Isotactic, Syndiotactic, and Atactic Polypropylenes Synthesized with Metallocene Catalysts. *Macromolecules* **1998**, *31*, 1335–1340. [CrossRef]
14. Wu, S.; Beckerbauer, R. Effect of Tacticity on Chain Entanglement in Poly(methyl methacrylate). *Polym. J.* **1992**, *24*, 1437–1442. [CrossRef]
15. Fetters, L.J.; Lohse, D.J.; Colby, R.H. Chain Dimensions and Entanglement Spacing. In *Physical Properties of Polymers. Handbook*, 2nd ed.; Mark, J.E., Ed.; Springer Science: New York, NY, USA, 2007; Chapter 25; pp. 447–454.
16. Pawlak, A. The Entanglements of Macromolecules and Their Influence on the Properties of Polymers. *Macromol. Chem. Phys.* **2019**, *220*, 1900043. [CrossRef]
17. Bu, H.S.; Gu, F.M.; Bao, L.; Chen, M. Influence of entanglements on crystallization of macromolecules. *Macromolecules* **1998**, *31*, 7108–7110. [CrossRef]

18. Teng, C.; Gao, Y.; Wang, X.; Jiang, W.; Zhang, C.; Wang, R.; Zhou, D.; Xue, G. Reentanglement Kinetics of Freeze-Dried Polymers above the Glass Transition Temperature. *Macromolecules* **2012**, *45*, 6648–6651. [CrossRef]

19. Liu, X.T.; Bao, R.Y.; Li, Y.M.; Yang, W.; Xie, B.H.; Yang, M.B. Effect of chain entanglement on the melt-crystallization behavior of poly(L-lactide) acid. *J. Polym. Res.* **2016**, *23*, 164. [CrossRef]

20. Plazek, D.J.; Raghupathi, N.; O'Rourke, V.M. New evidence for molecular entanglements. *J. Polym. Sci. Part B Polym. Phys.* **1980**, *18*, 1837–1846. [CrossRef]

21. Sasaki, T.; Morino, D.; Tabata, N. Origin of enhanced cold crystallization rate for freeze-dried poly(L-lactide) from solutions. *Polym. Eng. Sci.* **2011**, *51*, 1858–1865. [CrossRef]

22. Liu, C.-Y.; Morawetz, H. Kinetics of the Unfolding of Collapsed Polystyrene Chains above the Glass Transition Temperature. *Macromolecules* **1988**, *21*, 515–518. [CrossRef]

23. Pandey, A.; Champouret, Y.; Rastogi, S. Heterogeneity in the Distribution of Entanglement Density during Polymerization in Disentangled Ultrahigh Molecular Weight Polyethylene. *Macromolecules* **2011**, *44*, 4952–4960. [CrossRef]

24. Zhang, Y.; Chen, J.; Fu, Q.; Zhang, J. Novel Strategy to Improve the Performance of Poly(L-lactide): The Synergistic Effect of Disentanglement and Strong Shear Field. *ACS Sustain. Chem. Eng.* **2023**, *11*, 9630–9642. [CrossRef]

25. Wang, B.; Cavallo, D.; Zhang, X.; Zhang, B.; Chen, J. Evolution of chain entanglements under large amplitude oscillatory shear flow and its effect on crystallization of isotactic polypropylene. *Polymer* **2020**, *186*, 121899. [CrossRef]

26. Liu, M.; Chen, J.; Luo, J.; Min, J.; Fu, Q.; Zhang, J. Investigating the disentanglement of long chain branched polypropylene under different shear fields. *J. Appl. Polym. Sci.* **2022**, *139*, 51642. [CrossRef]

27. Kamkar, M.; Salehiyan, R.; Goudoulas, T.B.; Abbasi, M.; Saengow, C.; Erfanian, E.; Sadeghi, S.; Natale, G.; Rogers, S.A.; Giacomin, A.J.; et al. Large amplitude oscillatory shear flow: Microstructural assessment of polymeric systems. *Prog. Polym. Sci.* **2022**, *132*, 101580. [CrossRef]

28. Wang, S.-Q.; Ravindranath, S.; Wang, Y.; Boukany, P. New theoretical considerations in polymer rheology: Elastic break-down of chain entanglement network. *J. Chem. Phys.* **2007**, *127*, 064903. [CrossRef] [PubMed]

29. Kalb, B.; Pennings, A.J. Maximum strength and drawing mechanism of hot drawn high molecular weight polyethylene. *J. Mater. Sci.* **1980**, *15*, 2584–2590. [CrossRef]

30. Liang, T.N.; Zhang, Z.-G.; Li, T.; Yang, X.-Z. Interpenetration of two polymer chain globules. *Polymer* **2004**, *45*, 1365–1371. [CrossRef]

31. Sun, B.; Lu, Y.; Ni, H.; Wang, C. Highly crystallizable poly(ethylene terephthalate) prepared by freeze-extracting solutions. *Polymer* **1998**, *39*, 159–163. [CrossRef]

32. Huang, D.H.; Yang, Y.; Zhuang, G.; Li, B. Influence of Entanglements on the Glass Transition and Structural Relaxation Behaviors of Macromolecules. 1. Polycarbonate. *Macromolecules* **1999**, *32*, 6675–6678. [CrossRef]

33. Xie, Z.P.; Liu, D.; Zhu, P.P.; Yang, H.Y. Crystallization behavior of chain-disentangled poly(ethylene terephthalate). *Acta Polym. Sin.* **2010**, *5*, 522–529. [CrossRef]

34. Bernazzani, P.; Simon, S.L.; Plazek, D.J.; Ngai, K.L. Effects of entanglement concentration on Tg and local segmental motions. *Eur. Phys. J. E* **2002**, *8*, 201–207. [CrossRef]

35. Ajji, A.; Carreau, P.J.; Schreiber, H.P.; Rudin, A. Chain entanglement and viscoelastic properties of molten polymers. *J. Polym. Sci. Part B Polym. Phys.* **1986**, *24*, 1983–1990. [CrossRef]

36. Bastiaansen, C.W.M.; Meyer, H.E.H.; Lemstra, P.J. Memory effects in polyethylenes: Influence of processing and crystallization history. *Polymer* **1990**, *31*, 1435–1440. [CrossRef]

37. Wang, X.H.; Liu, R.; Wu, M.; Wang, Z.; Huang, Y. Effect of chain disentanglement on melt crystallization behaviour of isotactic polypropylene. *Polymer* **2009**, *50*, 5824–5827. [CrossRef]

38. Ogita, T.; Kawahara, Y.; Soga, Y.; Matsuo, M. Morphology and mechanical properties of ultrahigh molecular weight polypropylene prepared by gelation/crystallization at various temperatures. *Colloid Polym. Sci.* **1992**, *270*, 833–839. [CrossRef]

39. Pawlak, A.; Krajenta, J.; Galeski, A. The crystallization of polypropylene with reduced density of entanglements. *J. Polym. Sci. Part B Polym. Phys.* **2017**, *55*, 748–756. [CrossRef]

40. Bin, Y.; Tanabe, Y.; Nakabayashi, C.; Kurosu, H.; Matsuo, M. Morphology and mechanical properties of swollen gels and dry gel films of poly(vinyl alcohol) prepared by crystallization from solutions under simultaneous biaxially stretching. *Polymer* **2001**, *42*, 1183–1200. [CrossRef]

41. Huang, Y.F.; Xu, J.Z.; Zhang, Z.C.; Xu, L.; Li, L.B.; Li, J.F.; Li, Z.M. Melt processing and structural manipulation of highly linear disentangled ultrahigh molecular weight polyethylene. *Chem. Eng. J.* **2017**, *315*, 132–141. [CrossRef]

42. Westfahl, H., Jr.; Cardoso, M.B. Accessing the hidden lamellar nanostructure of semi-crystalline nascent polymers by small-angle X-ray scattering contrast variation. *J. Appl. Crystall.* **2011**, *44*, 1123–1126. [CrossRef]

43. Ronca, S.; Forte, G.; Tjaden, H.; Yao, Y.; Rastogi, S. Tailoring molecular structure via nanoparticles for solvent-free processing of ultra-high molecular weight polyethylene composites. *Polymer* **2012**, *53*, 2897–2907. [CrossRef]

44. Romano, D.; Tops, N.; Andablo-Reyes, E.; Ronca, S.; Rastogi, S. Influence of Polymerization Conditions on Melting Kinetics of Low Entangled UHMWPE and Its Implications on Mechanical Properties. *Macromolecules* **2014**, *47*, 4750–4760. [CrossRef]

45. Spronck, M.; Klein, A.; Blom, B.; Romano, D. Synthesis of Disentangled Ultra-High Molecular Weight Polyethylene using Vanadium(V)-Based Catalysts. *Z. Anorg. Allg. Chem.* **2018**, *644*, 993–998. [CrossRef]

46. Chen, Y.; Liang, P.; Yue, Z.; Li, W.; Dong, C.; Jiang, B.; Wang, J.; Yang, Y. Entanglement Formation Mechanism in the POSS Modified Heterogeneous Ziegler–Natta Catalysts. *Macromolecules* **2019**, *52*, 7593–7602. [CrossRef]

47. Pandey, A.; Toda, A.; Rastogi, S. Influence of Amorphous Component on Melting of Semicrystalline Polymers. *Macromolecules* **2011**, *44*, 8042–8055. [CrossRef]

48. Chammingkwan, P.; Bando, Y.; Mai, L.T.T.; Wada, T.; Thakur, A.; Terano, M.; Sinthusai, L.; Taniike, T. Less Entangled Ultrahigh-Molecular-Weight Polyethylene Produced by Nano-Dispersed Ziegler–Natta Catalyst. *Ind. Eng. Chem. Res.* **2021**, *60*, 2818–2827. [CrossRef]

49. Forte, G.; Ronca, S. Synthesis of Disentangled Ultra-High Molecular Weight Polyethylene: Influence of Reaction Medium on Material Properties. *Int. J. Polym. Sci.* **2017**, *2017*, 7431419. [CrossRef]

50. Ibar, J.P. Processing Polymer Melts under Rheo-Fluidification Flow Conditions, Part 1: Boosting Shear-Thinning by Adding Low Frequency Nonlinear Vibration to Induce Strain Softening. *J. Macromol. Sci. B. Phys.* **2013**, *52*, 407–441. [CrossRef]

51. Chen, K.-Y.; Zhou, N.-Q.; Liu, B.; Jin, G. Improved Mechanical Properties and Structure of Polypropylene Pipe Prepared under Vibration Force Field. *J. Appl. Polym. Sci.* **2009**, *114*, 3612–3620. [CrossRef]

52. An, F.Z.; Gao, X.Q.; Lei, J.; Deng, C.; Li, Z.M.; Shen, K.Z. Vibration assisted extrusion of polypropylene. *Chin. J. Polym. Sci.* **2015**, *33*, 688–696. [CrossRef]

53. Isayev, A.I.; Wong, C.M.; Zeng, X. Effect of oscillations during extrusion on rheology and mechanical properties of polymers. *Adv. Polym. Technol.* **1990**, *10*, 31–45. [CrossRef]

54. Lin, W.; Yang, Z.T.; Qu, J.-P. Short-time fabrication of well-mixed high-density polyethylene/ultrahigh-molecular-weight polyethylene blends under elongational flow: Morphology, mechanical properties and mechanism. *Polym. Int.* **2019**, *68*, 904–914. [CrossRef]

55. Wang, Y.; Liu, M.; Chen, J.; Luo, J.; Min, J.; Fu, Q.; Zhang, J. Efficient disentanglement of polycarbonate melts under complex shear field. *Polymer* **2020**, *201*, 122610. [CrossRef]

56. Lin, Y.-H.; Juang, J.H. Onset of Entanglement. *Macromolecules* **1999**, *32*, 181–185. [CrossRef]

57. De Gennes, P.G. Reptation of a polymer chain in the presence of fixed obstacles. *J. Chem. Phys.* **1971**, *55*, 572–579. [CrossRef]

58. Doi, M.; Edwards, S.F. Dynamics of concentrated polymer systems. Part 1—Brownian motion in the equilibrium state. *J. Chem. Soc. Faraday Trans. 2* **1978**, *74*, 1789–1801. [CrossRef]

59. Zulli, F.; Giordano, M.; Andreozzi, L. Onset of entanglement and reptation in melts of linear homopolymers: Consistent rheological simulations of experiments from oligomers to high polymers. *Rheol. Acta* **2015**, *54*, 185–205. [CrossRef]

60. Talebi, S. Disentangled Polyethylene with Sharp Molar Mass Distribution: Implications for Sintering. Ph.D. Thesis, Technische Universiteit Eindhoven, Eindhoven, The Netherlands, 2008.

61. Darabi, E.; Itskov, M. A generalized tube model of rubber elasticity. *Soft Matter* **2021**, *17*, 1675–1684. [CrossRef] [PubMed]

62. Robertson, C.G.; Warren, S.; Plazek, D.J.; Roland, C.M. Reentanglement kinetics in sheared polybutadiene solutions. *Macromolecules* **2004**, *37*, 10018–10022. [CrossRef]

63. Costanzo, S.; Huang, Q.; Ianniruberto, G.; Marrucci, G.; Hassager, O.; Vlassopoulos, D. Shear and extensional rheology of polystyrene melts and solutions with the same number of entanglements. *Macromolecules* **2016**, *49*, 3925–3935. [CrossRef]

64. Likhtman, A.E.; McLeish, T.C.B. Quantative theory for linear dynamics of linear entangled polymers. *Macromolecules* **2002**, *35*, 6332–6343. [CrossRef]

65. Van Ruymbeke, E.; Keunings, R.; Stephenne, V.; Hagenaars, A.; Bailly, C. Evaluation of reptation models for predicting the linear viscoelastic properties of entangled linear polymers. *Macromolecules* **2002**, *35*, 2689–2699. [CrossRef]

66. Leygue, A.; Bailly, C.; Keunings, R. A differential tube-based model for predicting the linear viscoelastic moduli of polydisperse entangled linear polymers. *J. Non Newton. Fluid Mech.* **2006**, *133*, 28–34. [CrossRef]

67. Doi, M. Explanation for the 3.4 power law of viscosity of polymeric liquids on the basis of the tube model. *J. Polym. Sci. B Polym. Phys.* **1983**, *21*, 667–684. [CrossRef]

68. Baig, C.; Mavrantzas, V.G. From atomistic trajectories to primitive paths to tube models: Linking atomistic simulations with the reptation theory of polymer dynamics. *Soft Matter* **2010**, *6*, 4603–4612. [CrossRef]

69. Marrucci, G. Relaxation by reptation and tube enlargement: A model for polydisperse polymers. *J. Polym. Sci. B Polym. Phys.* **1985**, *23*, 159–177. [CrossRef]

70. Marrucci, G.; Inanniruberto, G. Interchain pressure effect in extensional flows of entangled polymer melts. *Macromolecules* **2004**, *37*, 3934–3942. [CrossRef]

71. Van Ruymbeke, E.; Keunings, R.; Bailly, C. Prediction of linear viscoelastic properties for polydisperse mixtures of entangled star and linear polymers: Modified tube-based model and comparison with experimental results. *J. Non Newton. Fluid Mech.* **2005**, *128*, 7–22. [CrossRef]

72. Larson, R.G. Combinatorial rheology of branched polymer melts. *Macromolecules* **2001**, *34*, 4556–4571. [CrossRef]

73. Vandoolaeghe, W.L.; Kutter, S.; Terentjev, E.M. Two tube models of rubber elasticity. *J. Polym. Sci. Part B Polym. Phys.* **2006**, *44*, 2679–2697. [CrossRef]

74. Hopmann, C.; Twardowski, B.; Bakir, C. Limitations of Reptation Theory for Modeling the Stress-Dependent Rheological Behavior of Polyethylene Terephthalate above the Glass-Transition Temperature. *Polym. Eng. Sci.* **2020**, *60*, 765–772. [CrossRef]

75. Barham, P.J.; Sadler, D.M. A neutron scattering study of the melting behavior of polyethylene single crystals. *Polymer* **1991**, *32*, 393–395. [CrossRef]

76. Das, C.; Read, D.J. A tube model for predicting the stress and dielectric relaxations of polydisperse linear polymers. *J. Rheol.* **2023**, *67*, 693–721. [CrossRef]

77. McLeish, T.C.B. Tube theory of entangled polymer dynamics. *Adv. Phys.* **2002**, *51*, 1379–1527. [CrossRef]

78. Richter, D.; Kruteva, M. Polymer dynamics under confinement. *Soft Matter* **2019**, *15*, 7316–7349. [CrossRef] [PubMed]

79. Richter, D. Neutron scattering in polymer physics. *Physica B* **2000**, *276–278*, 22–29. [CrossRef]

80. Kirste, R.G.; Kruse, W.A.; Schelten, J. Die Bestimmung des Trägheitsradius von Polymethylmethacrylat in Glaszustand durch Neutronenbeugung. *Die Makromol. Chem.* **1973**, *162*, 299–303. [CrossRef]

81. Schelten, J.; Wignall, G.D.; Ballard, D.G.H.; Schmatz, W. Neutron small-angle scattering by mixtures of H and D-tagged molecules of polystyrene and polyethylene. *Colloid Polym. Sci.* **1974**, *252*, 749–752. [CrossRef]

82. Sperling, H. *Introduction to Physical Polymer Science*, 4th ed.; John Wiley and Sons: Hoboken, NJ, USA, 2006; p. 203.

83. Higgins, J.S.; Stein, R.S. Recent developments in polymer applications of small-angle neutron, X-ray and light scattering. *J. Appl. Cryst.* **1978**, *11*, 346–375. [CrossRef]

84. Michler, G.H. *Atlas of Polymer Structure: Morphology, Deformation and Fracture Structures*; Carl Hanser Verlag: Munich, Germany, 2016; p. 9.

85. Ewen, B.; Richter, D. Neutron Spin Echo Investigations on the segmental Dynamics of Polymer in Melts, Networks and Solutions. *Adv. Polym. Sci.* **1997**, *134*, 1–130.

86. Colmenero, J.; Arbe, A. Recent Progress on Polymer Dynamics by Neutron scattering: From Simple Polymer to Complex Materials. *J. Polym. Sci. Polym. Phys.* **2013**, *51*, 87–113. [CrossRef]

87. Schleger, P.; Farago, B.; Lartigue, C.; Kollmar, A.; Richter, D. Clear evidence of reptation in polyethylene from neutron spin-echo spectroscopy. *Phys. Rev. Lett.* **1998**, *81*, 124. [CrossRef]

88. Oeser, R.; Ewen, B.; Richter, D.; Farago, B. Dynamic fluctuations of crosslinks in a rubber: A neutron-spin-echo study. *Phys. Rev. Lett.* **1988**, *60*, 1041–1044. [CrossRef]

89. Ma, J.; Carillo, J.-M.Y.; Do, C.; Chen, W.-R.; Falus, P.; Shen, Z.; Hong, K.; Sumpter, B.G.; Wang, Y. Spatial correlations of entangled polymer dynamics. *Phys. Rev. E* **2021**, *104*, 024503. [CrossRef] [PubMed]

90. Arbe, A.; Alvarez, F.; Colmenero, J. Insight into the Structure and Dynamics of Polymers by Neutron Scattering Combined with Atomistic Molecular Dynamics Simulations. *Polymers* **2020**, *12*, 3067. [CrossRef] [PubMed]

91. Richter, D.; Monkenbusch, M.; Arbe, A.; Colmenero, J. Neutron Spin Echo in Polymer Systems. *Adv. Polym. Sci.* **2005**, *174*, 1–221. [CrossRef]

92. Genix, A.-C.; Oberdisse, J. Structure and dynamics of polymer nanocomposites studied by X-ray and neutron scattering techniques. *COCIS* **2015**, *20*, 293–303. [CrossRef]

93. Bhowmik, D.; Pomposo, J.A.; Juranyi, F.; García-Sakai, V.; Zamponi, M.; Su, Y.; Arbe, A.; Colmenero, J. Microscopic dynamics in nanocomposites of poly(ethylene oxide) and poly(methyl methacrylate) soft nanoparticles: A quasi-elastic neutron scattering study. *Macromolecules* **2014**, *47*, 304–315. [CrossRef]

94. Schneider, G.J.; Nusser, K.; Willner, L.; Falus, P.; Richter, D. Dynamics of entangled chains in polymer nanocomposites. *Macromolecules* **2011**, *44*, 5857–5860. [CrossRef]

95. Nusser, K.; Schneider, G.J.; Richter, D. Microscopic origin of the terminal relaxation time in polymer nanocomposites: An experimental precedent. *Soft Matter* **2011**, *7*, 7988–7991. [CrossRef]

96. Kong, D.-H.; Yang, M.-H.; Zhang, X.-S.; Du, Z.-C.; Fu, Q.; Gao, X.-Q.; Gong, J.W. Control of Polymer Properties by Entanglement: A Review. *Macromol. Mater. Eng.* **2021**, *306*, 2100536. [CrossRef]

97. Wu, S. Chain structure an entanglement. *J. Polym. Sci. Polym. Phys.* **1989**, *27*, 723–741. [CrossRef]

98. Dorgan, J.R.; Janzen, J.; Clayton, M.P.; Hait, S.B.; Knauss, D.M. Melt rheology of variable L-content poly(lactic acid). *J. Rheol.* **2005**, *49*, 607–619. [CrossRef]

99. Niu, H.; Wang, Y.; Liu, X.; Wang, Y.; Li, Y. Determination of plateau moduli and entanglement molecular weights of ultra-high molecular weight isotactic polypropylene synthesized by Ziegler-Natta catalyst. *Polym. Test.* **2017**, *60*, 260–265. [CrossRef]

100. Wu, S. Dynamic rheology and molecular weight distribution of insoluble polymers: Tetrafluoroethylene-hexafluoropropylene copolymers. *Macromolecules* **1985**, *18*, 2023–2030. [CrossRef]

101. Raju, V.R.; Menezes, E.V.; Marin, G.; Graessley, W.W.; Fetter, L.J. Concentration and molecular weight dependence of viscoelastic properties in linear and star polymers. *Macromolecules* **1981**, *14*, 1668–1676. [CrossRef]

102. Pogodina, N.V.; Winter, H.H. Polypropylene Crystallization as a Physical Gelation Process. *Macromolecules* **1998**, *31*, 8164–8172. [CrossRef]

103. Vega, J.F.; Rastogi, S.; Peters, G.W.M.; Meijer, H.E.H. Rheology and reptation of linear polymers. Ultrahigh molecular weight chain dynamics in the melt. *J. Rheol.* **2004**, *48*, 663–678. [CrossRef]

104. Li, N.; Zhang, Q.; Yang, Q.; Huang, Y.; Liao, X.; Zhao, W. The dependence time of melting behavior on rheological aspects of disentangled polymer melt: A route to the heterogeneous melt. *J. Polym. Res.* **2015**, *22*, 55. [CrossRef]

105. Nobile, M.R.; Cocchini, F. Evaluation of molecular weight distribution from dynamic moduli. *Rheol. Acta* **2001**, *40*, 111–119. [CrossRef]

106. Krajenta, J.; Safandowska, M.; Pawlak, A. The re-entangling of macromolecules in polypropylene. *Polymer* **2019**, *175*, 215–226. [CrossRef]

107. Martins, J.A.; Zhang, W.; Brito, A.M. Origin of the melt memory effect in polymer crystallization. *Polymer* **2010**, *51*, 4185–4194. [CrossRef]

108. Wang, S.Q. *Nonlinear Polymer Rheology. Macroscopic Phenomenology and Molecular Foundation*; John Wiley and Sons: Hoboken, NJ, USA, 2018; pp. 27–28.

109. Cheung, S.Y.; Wen, W.; Gao, P. Disentanglement and Micropore Structure of UHMWPE in an Athermal Solvent. *Polym. Eng. Sci.* **2014**, *55*, 1177–1186. [CrossRef]

110. Litvinov, V.M.; Ries, M.E.; Baughman, T.W.; Henke, A.; Matloka, P.P. Chain entanglements in polyethylene melts. Why is it studied again? *Macromolecules* **2013**, *46*, 541–547. [CrossRef]

111. Stern, C.; Frick, A.; Weickert, G. Relationship Between the Structure and Mechanical Properties of Polypropylene: Effects of the Molecular Weight and Shear-Induced Structure. *J. Appl. Polym. Sci.* **2007**, *103*, 519–533. [CrossRef]

112. Fetters, L.J.; Lohse, D.J.; Graessley, W.W. Chain dimensions and entanglement spacings in dense macromolecular systems. *J. Polym. Sci. Part B Polym. Phys.* **1999**, *37*, 1023–1033. [CrossRef]

113. Wu, S. Predicting chain conformation and entanglement of polymers from chemical structure. *Polym. Eng. Sci.* **1992**, *32*, 823–830. [CrossRef]

114. Aguilar, M.; Vega, J.F.; Sanz, E.; Martinez-Salazar, J. New aspects on the rheological behaviour of metallocene catalysed polyethylenes. *Polymer* **2001**, *42*, 9713–9721. [CrossRef]

115. Cooper-White, J.J.; Mackay, M.E. Rheological properties of poly(lactides). Effect of molecular weight and temperature on the viscoelasticity of poly(l-lactic acid). *J. Polym. Sci. Part B Polym. Phys.* **1999**, *37*, 1803–1814. [CrossRef]

116. Grijpma, D.W.; Penning, J.P.; Pennings, A.J. Chain entanglement, mechanical properties and drawability of poly(lactide). *Colloid Polym. Sci.* **1994**, *272*, 1068. [CrossRef]

117. Krajenta, J.; Safandowska, M.; Pawlak, A.; Galeski, A. All-polymer composites—A new approach with the use of disentangled semi-crystalline polymers. Part I. Disentangling and properties of disentangled polylactide. *Polimery* **2020**, *65*, 167–173. [CrossRef]

118. Chile, L.-E.; Mehrkhodavandi, P.; Hatzikiriakos, S.G. A Comparison of the Rheological and Mechanical Properties of Isotactic, Syndiotactic, and Heterotactic Poly(lactide). *Macromolecules* **2016**, *49*, 909–919. [CrossRef]

119. Fetters, L.J.; Lohse, D.J.; Richter, D.; Witten, T.A.; Zirkel, A. Connection between Polymer Molecular Weight, Density, Chain Dimensions, and Melt Viscoelastic Properties. *Macromolecules* **1994**, *27*, 4639–4647. [CrossRef]

120. Liu, C.; Yu, J.; He, J.; Liu, W.; Sun, C.; Jing, Z. A Reexamination of G_N^0 and Me of Syndiotactic Polypropylenes with Metallocene Catalysts. *Macromolecules* **2004**, *37*, 9279–9282. [CrossRef]

121. Huang, C.-L.; Chen, Y.-C.; Hsiao, T.-J.; Tsai, J.-C.; Wang, C. Effect of Tacticity on Viscoelastic Properties of Polystyrene. *Macromolecules* **2011**, *44*, 6155–6161. [CrossRef]

122. Stoclet, G.; Du Sart, G.G.; Yeniad, B.; De Vos, S.; Lefebvre, J.M. Isothermal crystallization and structural characterization of poly(ethylene-2,5-furanoate). *Polymer* **2015**, *72*, 165–175. [CrossRef]

123. Colby, R.H.; Fetters, L.J.; Graessley, W.W. Melt Viscosity-Molecular Weight Relationship for Linear Polymers. *Macromolecules* **1987**, *20*, 2226–2237. [CrossRef]

124. Fetters, L.H.; Lohse, D.J.; Garcia-Franco, C.A.; Brant, P.; Richter, D. Prediction of Melt State Poly(α-olefin) Rheological Properties: The Unsuspected Role of the Average Molecular Weight per Backbone Bond. *Macromolecules* **2002**, *35*, 10096–10101. [CrossRef]

125. Shan, W.; Xiao, K.; Thomas, E.L. Influence of Entanglements on Ultrahigh Strain Rate Deformation of Polystyrene Micro projectiles. *Macromolecules* **2022**, *55*, 9594–9600. [CrossRef]

126. Song, L. Effect of Entanglement Density on Mechanical Properties and Deformation Behavior of Rubber-Modified PVC/α-MSAN Blends. *Ind. Eng. Chem. Res.* **2013**, *52*, 12567–12573. [CrossRef]

127. Prest, W.M.; Porter, R.S. Rheological properties of poly(2,6-dimethylphenylene oxide)-polystyrene blends. *J. Polym. Sci. (A-2)* **1972**, *10*, 1639–1655. [CrossRef]

128. Van Melick, H.G.H.; Govaert, L.E.; Meijer, H.E.H. On the origin of strain hardening in glassy polymers. *Polymer* **2003**, *44*, 2493–2502. [CrossRef]

129. Hao, X.; Kaschta, J.; Liu, X.; Pan, Y.; Schubert, D.W. Entanglement network formed in miscible PLA/PMMA blends and its role in rheological and thermo-mechanical properties of the blends. *Polymer* **2015**, *80*, 38–45. [CrossRef]

130. Wu, S. Chain entanglement and melt viscosity of compatible polymer blends: Poly(methyl methacrylate) and poly(styrene-acrylonitrile). *Polymer* **1987**, *28*, 1144–1148. [CrossRef]

131. Wu, S. Entanglement, Friction and Free Volume between Dissimilar Chains in Compatible Polymer Blends. *J. Polym. Sci. B Polym. Phys.* **1987**, *25*, 2511–2529. [CrossRef]

132. Song, L.; Zhang, Y.; Ren, J.; Li, Y.; Yang, B.; Xing, E.; Wang, Y.; Shi, Y. Effect of Entanglement Density on Mechanical Properties and the Deformation Mechanism of Rubber-Modified PPO/PS Blends. *Macromol. Mater. Eng.* **2022**, *307*, 2200325. [CrossRef]

133. Xie, M.; Li, M. Viscosity reduction and disentanglement in ultrahigh molecular weight polyethylene melt: Effect of blending with polypropylene and poly(ethylene glycol). *Eur. Polym. J.* **2007**, *43*, 3480–3487. [CrossRef]

134. Chen, P.; Yang, H.; Chen, T.; Li, W. Weakly entangled ultrahigh molecular weight polyethylene prepared via ethylene extrusion polymerization. *Ind. Eng. Chem. Res.* **2015**, *54*, 11024–11032. [CrossRef]

135. Li, W.; Guan, C.; Xu, J.; Mu, J.; Gong, D.; Chen, Z.R.; Zhou, Q. Disentangled UHMWPE/POSS nanocomposites prepared by ethylene in situ polymerization. *Polymer* **2014**, *55*, 1792–1798. [CrossRef]

136. Drakopoulos, S.X.; Forte, G.; Ronca, S. Relaxation Dynamics in Disentangled Ultrahigh Molecular Weight Polyethylene via Torsional Rheology. *Ind. Eng. Chem. Res.* **2020**, *59*, 4515–4523. [CrossRef]

137. Guo, L.; Zhang, J.; Hu, J.; Du, X.; Cui, B. The effects of entanglement concentration on the hydrodynamic properties of cereal starches. *J. Sci. Food Agric.* **2017**, *97*, 2795–2802. [CrossRef]

138. Guo, L. Role of entanglement concentration in dynamic viscoelasticity and film-forming property of cereal starches. *Int. J. Biol. Macromol.* **2018**, *108*, 1357–1363. [CrossRef]

139. Mackay, M.E.; Dao, T.T.; Tuteja, A.; Ho, D.L.; Horn, B.V.; Kim, H.C.; Hawker, C.J. Nanoscale effects leading to non-Einstein-like decrease in viscosity. *Nat. Mater.* **2003**, *2*, 762–766. [CrossRef]

140. Chai, S.-C.; Xu, T.-Y.; Cao, X.; Wang, G.; Chen, Q.; Li, H.-L. Ultrasmall Nanoparticles Diluted Chain Entanglement in Polymer Nanocomposites. *Chin. J. Polym. Sci.* **2019**, *37*, 797–805. [CrossRef]

141. Nusser, K.; Schneider, G.J.; Pyckhout-Hintzen, W.; Richter, D. Viscosity decrease and reinforcement in polymer-silsesquioxane composites. *Macromolecules* **2011**, *44*, 7820–7830. [CrossRef]

142. Mangal, R.; Srivastava, S.; Archer, L.A. Phase stability and dynamics of entangled polymer-nanoparticle composites. *Nat. Commun.* **2015**, *6*, 7198. [CrossRef] [PubMed]

143. Senses, E.; Ansar, S.M.; Kitchens, C.L.; Mao, Y.; Narayanan, S.; Natarajan, B.; Faraone, A. Small Particle Driven Chain Disentanglements in Polymer Nanocomposites. *Phys. Rev. Lett.* **2017**, *118*, 147801. [CrossRef] [PubMed]

144. Zhang, X.; Zhao, S.; Xin, Z. The chain disentanglement effect of polyhedral oligomeric silsesquioxanes (POSS) on ultra-high molecular weight polyethylene (UHMWPE). *Polymer* **2020**, *202*, 122631. [CrossRef]

145. Sui, Y.; Yui, Y.; Wei, P.; Cong, C.; Meng, X.; Ye, H.-M.; Zhou, Q. Nanoscale effects of TiO$_2$ nanoparticles on the rheological behaviors of ultra-high molecular weight polyethylene (UHMWPE). *Soft Matter* **2023**, *19*, 5459–5467. [CrossRef] [PubMed]

146. Heidari, A.; Zarghami, H.; Talebi, S.; Rezaei, M. A disentangled state using TiCl$_4$/MgCl$_2$ catalyst: A case study of polyethylene. *Iran. Polym. J.* **2018**, *27*, 701–708. [CrossRef]

147. Fu, J.; Wang, Y.; Shen, K.; Fu, Q.; Zhang, J. Insight into Shear-Induced Modification for Improving Processability of Polymers: Effect of Shear Rate on the Evolution of Entanglement State. *J. Polym. Sci. B Polym. Phys.* **2019**, *57*, 598–606. [CrossRef]

148. Cao, Y.; Wu, Y.; Tang, X.; Zhou, Q.; Stapf, S.; Mattea, C.; Li, W. Long-term efficiency for reducing entanglements of nascent polyethylene by a polystyrene-modified Ziegler-Natta catalyst. *J. Appl. Polym. Sci.* **2022**, *39*, 51790. [CrossRef]

149. Liu, M.; Wang, Y.; Chen, J.; Luo, J.; Fu, Q.; Zhang, J. The retarded recovery of disentangled state by blending HDPE with ultra-high molecular weight polyethylene. *Polymer* **2020**, *192*, 122329. [CrossRef]

150. Wang, B.; Cavallo, D.; Chen, J. Delay of re-entanglement kinetics by shear-induced nucleation precursors in isotactic polypropylene melt. *Polymer* **2020**, *210*, 123000. [CrossRef]

151. Krajenta, J.; Pawlak, A.; Galeski, A. Deformation of disentangled polypropylene crystalline grains into nanofibers. *J. Polym. Sci. Part B Polym. Phys.* **2016**, *54*, 1983–1994. [CrossRef]

152. Lippits, D.R.; Rastogi, S.; Talebi, S.; Bailly, C. Formation of entanglements in initially disentangled polymer melts. *Macromolecules* **2006**, *39*, 8882–8885. [CrossRef]

153. Talebi, S.; Duchateau, R.; Rastogi, S.; Kaschta, J.; Peters, G.; Lemstra, P.J. Molar mass and molecular weight distribution determination of UHMWPE synthesized using a living homogeneous catalyst. *Macromolecules* **2010**, *43*, 2780–2788. [CrossRef]

154. Rastogi, S.; Kurelec, L.; Cuijpers, J.; Lippits, D.; Wimmer, M.; Lemstra, P.J. Disentangled state in polymer melts; a route to ultimate physical and mechanical properties. *Macromol. Mater. Eng.* **2003**, *288*, 964–970. [CrossRef]

155. Luo, J.; Liu, M.; Chen, J.; Min, J.; Fu, Q.; Zhang, J. Effectively maintaining the disentangled state of isotactic polypropylene in the presence of graphene nanoplatelet. *Polymer* **2021**, *226*, 23806. [CrossRef]

156. Luo, J.; Chen, J.; Liu, M.; Min, J.; Fu, Q.; Zhang, J. Investigating the Influence of Incorporation of Boron Nitride on the Kinetics of Isotactic Polypropylene Entanglement Recovery. *Ind. Eng. Chem. Res.* **2021**, *60*, 12901–12910. [CrossRef]

157. Slouf, M.; Krajenta, J.; Gajdosova, V.; Pawlak, A. Macro- and Micromechanical Properties of Polymers with Reduced Density of Entanglements. *Polym. Eng. Sci.* **2021**, *61*, 1773–1790. [CrossRef]

158. Schrauwen, B.A.G.; Janssen, R.P.M.; Govaert, L.E.; Meijer, H.E.H. Intrinsic deformation behavior of semicrystalline polymers. *Macromolecules* **2004**, *37*, 6069–6078. [CrossRef]

159. Meijer, H.W.H.; Govaert, L.E. Mechanical performance of polymer systems: The relation between structure and properties. *Prog. Polym. Sci.* **2005**, *30*, 915–938. [CrossRef]

160. Zuo, F.; Keum, J.K.; Chen, X.; Hsiao, B.S.; Chen, H.; Lai, S.Y.; Wevers, R.; Li, J. The role of interlamellar chain entanglement in deformation-induced structure changes during uniaxial stretching of isotactic polypropylene. *Polymer* **2007**, *48*, 6867–6880. [CrossRef]

161. Hobeika, S.; Men, Y.; Strobl, G. Temperature and Strain Rate Independence of Critical Strains in Polyethylene and Poly(ethylene-co-vinyl acetate). *Macromolecules* **2000**, *33*, 1827–1833. [CrossRef]

162. Fu, Q.; Men, Y.; Strobl, G. A molar mass induced transition in the yielding properties of linear polyethylene. *Polymer* **2003**, *44*, 1941–1947. [CrossRef]

163. Hong, K.; Rastogi, A.; Strobl, G. A Model Treating Tensile Deformation of Semicrystalline Polymers: Quasi-Static Stress–Strain Relationship and Viscous Stress Determined for a Sample of Polyethylene. *Macromolecules* **2004**, *37*, 10165–10173. [CrossRef]

164. Pawlak, A.; Galeski, A. Plastic Deformation of Crystalline Polymers: The Role of Cavitation and Crystal Plasticity. *Macromolecules* **2005**, *38*, 9688–9697. [CrossRef]

165. Pawlak, A.; Galeski, A. Cavitation during tensile drawing of annealed high density polyethylene. *Polymer* **2010**, *51*, 5771–5779. [CrossRef]

166. Men, Y.; Rieger, J.; Strobl, G. Role of the Entangled Amorphous Network in Tensile Deformation of Semicrystalline Polymers. *Phys. Rev. Lett.* **2003**, *91*, 095502. [CrossRef] [PubMed]

167. Haward, R.N. Strain Hardening of High Density Polyethylene. *J. Polym. Sci. Part B Polym. Phys.* **2007**, *45*, 1090–1099. [CrossRef]

168. Argon, A.S. Physical basis of distortional and dilatational plastic flow in glassy polymers. *J. Macromol. Sci. Phys.* **1973**, *8*, 573–596. [CrossRef]

169. Kramer, E.J. Open Questions in the Physics of Deformation of Polymer Glasses. *J. Polym. Sci. Part B Polym. Phys.* **2005**, *43*, 3369–3371. [CrossRef]

170. Hoy, R.S.; Robbins, M. Strain hardening of polymer glasses: Effect of entanglement density, temperature, and rate. *J. Polym. Sci. Part B Polym. Phys.* **2006**, *44*, 3487–3500. [CrossRef]

171. van Der Sanden, M.C.M. Ultimate Toughness of Amorphous Polymers. Ph.D. Thesis, Technische Universiteit Eindhoven, Eindhoven, The Netherlands, 1993.

172. Smith, P.; Lemstra, P.J.; Booij, H.C. Ultradrawing of high-molecular-weight polyethylene cast from solution. II. Influence of initial polymer concentration. *J. Polym. Sci. Polym. Phys. Ed.* **1981**, *19*, 887–888. [CrossRef]

173. Donald, A.M.; Kramer, E.J. Effects of molecular entanglements on craze microstructure in glassy polymers. *J. Polym. Sci. Polym. Phys. Ed.* **1982**, *20*, 899–909. [CrossRef]

174. Donald, A.M.; Kramer, E.J. The competition between shear deformation and crazing in glassy polymers. *J. Mater. Sci.* **1982**, *17*, 1871–1879. [CrossRef]

175. Garcia-Franco, C.A.; Harrington, B.A.; Lohse, D.J. On the rheology of ethylene–octene copolymers. *Rheol. Acta* **2005**, *44*, 591–599. [CrossRef]

176. Kennedy, M.A.; Peacock, A.J.; Mandelkern, L. Tensile properties of crystalline polymers: Linear polyethylene. *Macromolecules* **1994**, *27*, 5297–5310. [CrossRef]

177. Bartczak, Z.; Kozanecki, M. Influence of molecular parameters on high-strain deformation of polyethylene in the plane-strain compression. Part I. Stress-strain behavior. *Polymer* **2005**, *46*, 8210–8221. [CrossRef]

178. Arruda, E.M.; Boyce, M.C. A three-dimensional constitutive model for the large stretch behavior of rubber elastic materials. *J. Mech. Phys. Solids* **1993**, *41*, 389–412. [CrossRef]

179. Smith, P.; Lemstra, P.J. Ultra-drawing of high molecular weight polyethylene cast from solution. *Colloid Polym. Sci.* **1980**, *258*, 891–894. [CrossRef]

180. Lemstra, P.J.; Van Aerle, N.A.; Bastiaansen, C.W.M. Chain-Extended Polyethylene. *Polym. J.* **1987**, *19*, 85–98. [CrossRef]

181. Yeh, J.T.; Chang, S.S.; Wu, T.W. Effect of the ultradrawing behavior of gel films of ultrahigh-molecular-weight polyethylene and low-molecular-weight polyethylene blends on their physical properties. *J. Appl. Polym. Sci.* **2008**, *107*, 854–862. [CrossRef]

182. Ikeda, Y.; Ohta, T. The influence of chain entanglement density on ultra-drawing behavior of ultra-high-molecular-weight polypropylene in the gel-casting method. *Polymer* **2008**, *49*, 621–627. [CrossRef]

183. Huang, B.; Ito, M.; Kanamoto, T. Deformation mechanism of amorphous poly(ethylene terephthalate) as a function of molecular weight and entanglements. *Polymer* **1994**, *35*, 1210–1215. [CrossRef]

184. Pawlak, A.; Krajenta, A.; Galeski, A. Cavitation phenomenon and mechanical properties of partially disentangled polypropylene. *Polymer* **2018**, *151*, 15–26. [CrossRef]

185. Pawlak, A.; Galeski, A. Cavitation during Tensile Deformation of Polypropylene. *Macromolecules* **2008**, *41*, 2839–2851. [CrossRef]

186. Logunov, M.A.; Orekhov, N.D. The Role of Intermolecular Entanglements in the Formation of Nanosized Pores during Deformation of Polyethylene: Atomistic Modeling. *Polym. Sci. Ser. A* **2021**, *63*, 591–599. [CrossRef]

187. Yue, Z.; Wang, N.; Cao, Y.; Li, W.; Dong, C.-D. Reduced Entanglement Density of Ultrahigh-Molecular-Weight Polyethylene Favored by the Isolated Immobilization on the MgCl$_2$ (110) Plane. *Ind. Eng. Chem. Res.* **2020**, *59*, 3351–3358. [CrossRef]

188. Zhang, H.; Zhao, S.; Yu, X.; Xin, Z.; Ye, C.; Li, Z.; Xia, J. Nascent Particle Sizes and Degrees of Entanglement Are Responsible for the Significant Differences in Impact Strength of Ultrahigh Molecular Weight Polyethylene. *J. Polym. Sci. B Polym. Phys.* **2019**, *57*, 632–641. [CrossRef]

189. Chen, Y.; Tao, G.; Li, W.; Zhou, Q.; Shu, B.; Jiang, B.; Wang, J.; Yang, Y. The in situ synthesis of weakly entangled ultra-high-molecular weight polyethylene/polyethylene wax blends and its synergetic disentanglement effect on LLDPE reinforcement. *Polym. Adv. Technol.* **2022**, *33*, 3728–3739. [CrossRef]

190. Schirmeister, C.G.; Hees, T.; Dolynchuk, O.; Licht, E.H.; Thurn-Albrecht, T.; Muelhaupt, R. Digitally Tuned Multidirectional All-Polyethylene Composites via Controlled 1D Nanostructure Formation during Extrusion-Based 3D Printing. *ACS Appl. Polym. Mater.* **2021**, *3*, 1675–1686. [CrossRef]

191. Chen, Y.; Li, W.; Zhang, L.; Ye, C.; Tao, G.; Ren, C.; Jiang, B.; Wang, J.; Yang, Y. In Situ Synthesized Self-Reinforced HDPE/UHMWPE Composites with High Content of Less Entangled UHMWPE and High Gradient-Distributed Oriented Structures. *ACS Appl. Polym. Mater.* **2023**, *5*, 88–98. [CrossRef]

192. Tao, G.; Chen, Y.; Mu, J.; Zhang, L.; Ye, C.; Li, W. Exploring the entangled state and molecular weight of UHMWPE on the microstructure and mechanical properties of HDPE/UHMWPE blends. *J. Appl. Polym. Sci.* **2021**, *138*, 50741. [CrossRef]

193. Barangizi, H.; Krajenta, J.; Pawlak, A. The influence of entanglements of macromolecules on the mechanical and thermal properties of polylactide composites with carbon nanotubes. *Express Polym. Lett.* **2023**, *17*, 738–758. [CrossRef]

194. Jurczuk, K.; Galeski, A.; Piorkowska, E. All-polymer nanocomposites with nanofibrillar inclusions generated in situ during compounding. *Polymer* **2013**, *54*, 4617. [CrossRef]

195. Krajenta, J.; Pawlak, A. The all-polymer composites and blends made of ethylene-octene copolymer and partially disentangled polypropylene using a new processing approach. *J. Appl. Polym. Sci.* **2024**, *141*, e55681. [CrossRef]